Glucose in a final 12% solution containing KCl (0.5 μmol/kg/min) were infused at a rate of 0.033 mmol/kg/min [6 mg/kg/min] through an antecubital vein via a constant infusion pump. Blood samples were drawn routinely at 0 and 120 min (9:00 and 11:00 a.m.) for determination of glucose and insulin. Value of glucose at 120 min (SSPG) was used as a marker of insulin sensitivity to glucose utilization. High SSPG levels indicate peripheral insulin resistance. At 120 min SSPG was rapidly measured using a Glucometer (Bayer Corporation, Osaka, Japan) separate from the usual measurement of glucose and insulin. When rapidly measured, if SSPG was found to be lower than 250 mg/dl, oral glucose intake was necessary to prevent hypoglycemia after the insulin sensitivity test. The subjects should have lunch within 30 min after the insulin sensitivity test to prevent hypoglycemia. Homeostasis model assessment (HOMA-IR) was calculated from fasting glucose and insulin concentrations during insulin sensitivity test as follows: HOMA-IR = fasting glucose (mg/dl) × fasting insulin (μU/ml)/405.

2.3. Statistical analysis

Values are expressed as mean ± S.E. A probability value of <0.05 was considered to indicate statistical significance. The strength of the correlation between FMD and GTN with respect to risk factors was assessed by Pearson's linear correlation and multiple regression analysis. The effects of pioglitazone on each clinical parameter were assessed by paired t-test and Pearson's linear correlation.

3. Results

3.1. Association between endothelial dysfunction and each parameter in 48 subjects

A significant inverse correlation was observed between FMD and SSPG ($r = -0.462$, $p < 0.001$; Fig. 1). There was no relation between FMD and HbA_{1c} ($p = 0.856$). We also observed a significant inverse correlation between FMD and systolic blood pressure ($r = -0.360$, $p < 0.013$). No significant correlation was found between FMD and diabetic duration, diastolic blood pressure, total cholesterol, HDL cholesterol, triglyceride, age or BMI. There was no relationship between FMD and HOMA-IR ($p = 0.097$).

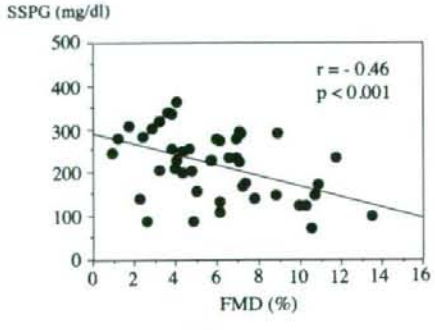

Fig. 1. Relationship between FMD and SSPG in subjects with type 2 diabetes. FMD, flow-mediated vasodilation; SSPG, steady state plasma glucose.

We performed multiple regression analysis to evaluate the independent influence of risk factors including SSPG, systolic blood pressure, HbA_{1c}, total cholesterol, BMI and age on FMD. FMD was independently related to SSPG (regression coefficient: $\beta = -0.419$, $p = 0.0086$) but not to systolic blood pressure ($\beta = -0.254$, $p = 0.0782$), HbA_{1c} ($\beta = -0.090$, $p = 0.5616$), total cholesterol ($\beta = -0.067$, $p = 0.6336$), BMI ($\beta = -0.258$, $p = 0.0863$) or age ($\beta = -0.085$, $p = 0.5650$).

With respect to GTN, no significant correlation was observed between GTN and SSPG or other parameters, including HbA_{1c}, diabetic duration, systolic blood pressure, diastolic blood pressure, total cholesterol, HDL cholesterol, triglyceride, age or BMI.

3.2. Effects of pioglitazone treatment on endothelial function and insulin resistance

The effects of treatment with pioglitazone were assessed in 10 male subjects with type 2 diabetes (a subgroup of 48 subjects). Table 1 shows the clinical parameters of the 10 subjects before and after pioglitazone treatment. SSPG, HbA_{1c} and fasting plasma glucose decreased and FMD increased significantly due to pioglitazone treatment. However, BMI, total cholesterol, HDL-cholesterol, triglyceride, systolic blood pressure and diastolic blood pressure did not

Table 1
Clinical characteristics of the subjects with type 2 diabetes treated with pioglitazone

	Before Tx	After Tx
Number	10	
Age (years)	65 ± 2	
SSPG (mg/dl)	230 ± 13	185 ± 17*
FMD (%)	4.5 ± 1.1	8.1 ± 1.5***
Body mass index (kg/m^2)	24.4 ± 0.4	24.7 ± 0.4
Fasting plasma glucose (mg/dl)	162 ± 11	133 ± 8*
HbA_{1c} (%)	8.4 ± 0.4	7.0 ± 0.3**
Total cholesterol (mg/dl)	199 ± 8	206 ± 7
HDL cholesterol (mg/dl)	47 ± 4	50 ± 4
Triglyceride (mg/dl)	120 ± 15	129 ± 13
Systolic blood pressure (mmHg)	137 ± 5	137 ± 2
Diastolic blood pressure (mmHg)	78 ± 5	79 ± 1

Values are mean ± S.E. *$p < 0.05$, **$p < 0.01$, ***$p < 0.001$ vs. before Tx. Tx, Treatments with pioglytazone.

significantly change. GTN was also not significantly altered.

The change in FMD before and after administration of pioglitazone was not significantly correlated with the change in HbA_{1c} ($p = 0.314$) or fasting plasma glucose ($p = 0.717$). The increase in FMD, that is, the improvement in endothelial function, was significantly correlated with the decrease in SSPG ($r = -0.649$, $p < 0.05$).

4. Discussion

In this study we found that vascular endothelial dysfunction was associated with insulin resistance in type 2 diabetes. This result was supported by the effects of the insulin sensitizer, pioglitazone, which improved both endothelial dysfunction and insulin resistance in patients with type 2 diabetes.

The close association between insulin resistance and endothelial dysfunction is our main interest. In a study by Hogikyan et al. [3], insulin resistance as measured by the insulin sensitivity index (minimal model: S_I), was not found to be correlated with endothelial dysfunction in subjects with type 2 diabetes. They measured the forearm blood flow (FABF) using venous occlusion plethysmography and used the FABF response to acetylcholine as an index of endothelial function. The narrow range of S_I values among the subjects might have led to the lack of a relationship between S_I and endothelial dysfunction. In addition, the sensitivity of the techniques using plethysmography might have been low.

Balletshofer et al. [12] reported a significant association between endothelial dysfunction and insulin resistance, as measured by the glucose clamp method, in young normotensive and normoglycemic first-degree relatives of patients with type 2 diabetes. Therefore, this association was observed in a non-diabetic population at future risk of type 2 diabetes.

Insulin causes endothelium-derived nitric oxide (NO)-dependent vasodilation [13]. It is suggested that this insulin action occurs via the phosphatidylinositol 3-kinase and Akt pathway [14,15]. As for insulin action, phosphatidylinositol 3-kinase activation is critical for insulin-mediated glucose uptake into skeletal muscle [16]. Therefore, insulin resistance due to a systemic defect in the phosphatidylinositol 3-kinase pathway might cause a combined defect in insulin-mediated glucose uptake and insulin-mediated endothelial vasodilation.

Among the risk factors for atherosclerosis, insulin resistance was found to be the sole predictor of endothelium dependent vasodilation by multiple regression analysis in the present study. We observed no relationship between FMD and HbA_{1c}. Bagg et al. found that a short-term reduction of HbA_{1c} levels did not appear to affect endothelial function in patients with type 2 diabetes [17]. Furthermore, Mather et al. reported that insulin resistance was the sole predictor of endothelial dysfunction following metformin treatment in type 2 diabetes in stepwise multivariate analysis, and HbA_{1c} and glucose levels were not significant predictors of endothelial dysfunction [18].

Treatment with HMG-CoA inhibitors (statins) has been shown to improve endothelial dysfunction [19–21]. Therefore, statin treatment may have affected the relationship between FMD and risk factors in the present study. In 48 diabetic subjects, 5 were treated with pravastatin and one with simvastatin. We performed statistical analysis in 42 subjects without statin treatment. There was a significant inverse correlation between SSPG and FMD ($r = -0.538$, $p < 0.001$). A significant inverse correlation was observed between FMD and systolic blood pressure ($r = -0.330$, $p < 0.05$). No significant correlation was found between FMD and HbA_{1c}, diabetic duration, diastolic blood pressure, total cholesterol, HDL cholesterol, triglyceride, age or BMI. On multiple regression analysis, FMD was independently related to SSPG (regression coefficient: $\beta = -0.500$, $p = 0.0032$) but not to systolic blood pressure, HbA_{1c}, total cholesterol, BMI or age.

Smoking is associated with endothelial dysfunction [22,23]. Smoking might interfere in the relationship between FMD and risk factors. In 48 diabetic subjects, 13 were smokers in the present study. Statistical analysis was performed in 35 non-smokers. A significant correlation was found between SSPG and FMD ($r = -0.582$, $p < 0.001$). There was a significant inverse correlation between FMD and systolic blood pressure ($r = -0.357$, $p < 0.05$). No significant correlation was observed between FMD and HbA_{1c}, diabetic duration, diastolic blood pressure, total cholesterol, HDL cholesterol, triglyceride, age or BMI. On multiple regression analysis, FMD was independently related to SSPG (regression coefficient: $\beta = -0.591$, $p = 0.0019$) but not to systolic blood pressure, HbA_{1c}, total cholesterol, BMI or age. In the present study, FMD did not correlate with HOMA-IR. SSPG is a more sensitive marker to measure insulin sensitivity than HOMA-IR.

Endothelial dysfunction and insulin resistance were improved by pioglitazone treatment in the present study. SSPG, HbA_{1c} and fasting plasma glucose were decreased and other risk factors were not changed by the treatment. It was reported that hyperglycemia itself inhibits endothelial NO synthase activity [24] and causes endothelial dysfunction [25]. On the other hand,

insulin resistance was also associated with endothelial dysfunction in 48 subjects with type 2 diabetes in this study. The change in FMD before and after treatment with pioglitazone was not significantly correlated with the change in HbA_{1c} or fasting plasma glucose, and the increase in FMD was significantly correlated with the decrease in SSPG in this study. Because of the small number of subjects ($n = 10$), we cannot exclude the possibility that the decreased plasma glucose level improved endothelial dysfunction. The decrease in plasma glucose level might be associated with improved endothelial function if the pioglitazone study was performed with more cases. It can at least be said that insulin resistance is an important factor affecting endothelial function. As previously described, a similar study [18] found that treatment with metformin improved both endothelial function and insulin resistance, and the glucose level and HbA_{1c} were not significant predictors of endothelial dysfunction. Considering generally than the above-mentioned points, it is suggested that increased insulin sensitivity plays an important role in the improvement of endothelial function by pioglitazone treatment.

Pistrosch et al. [26] demonstrated that treatment with rosiglitazone, another PPARγ activator, ameliorated insulin resistance measured by glucose clamp method, and improved endothelial function determined by venous occlusion plethysmography in patients with recently diagnosed type 2 diabetes. They performed a double-blind cross-over trial and treated with rosiglitazone and nateglinide in random order. Glycemic control was comparable under rosiglitazone and nateglinide. Only rosiglitazone improved insulin resistance and endothelial function in the study. Thus, they also showed the relation between insulin sensitivity and endothelial function independent of glucose level in type 2 diabetes.

In conclusion, in the present study we demonstrated significant association between vascular endothelial dysfunction and insulin resistance in type 2 diabetes, and pioglitazone treatment improved both endothelial dysfunction and insulin resistance with a statistical link. These data support the concept of the important role of insulin resistance in the pathogenesis of endothelial dysfunction in type 2 diabetes mellitus.

References

[1] S.B. Williams, J.A. Cusco, M.A. Roddy, M.T. Johnstone, M.A. Creager, Impaired nitric oxide-mediated vasodilation in patients with non-insulin-dependent diabetes mellitus, J. Am. Coll. Cardiol. 27 (1996) 567–574.

[2] A. Avogaro, F. Piarulli, A. Valerio, M. Miola, M. Calveri, P. Pavan, et al., Forearm nitric oxide balance, vascular relaxation, and glucose metabolism in NIDDM patients, Diabetes 46 (1997) 1040–1046.

[3] R.V. Hogikyan, A.T. Galecki, B. Pitt, J.B. Halter, D.A. Greene, M.A. Supiano, Specific impairment of endothelium-dependent vasodilation in subjects with type 2 diabetes independent of obesity, J. Clin. Endocrinol. Metab. 83 (1998) 1946–1952.

[4] M.A. Creager, T.F. Luscher, F. Cosentino, J.A. Beckman, Diabetes and vascular disease: pathophysiology, clinical consequences, and medical therapy: part I, Circulation 108 (2003) 1527–1532.

[5] K. Shinozaki, M. Suzuki, M. Ikebuchi, Y. Hara, Y. Harano, Demonstration of insulin resistance in coronary heart disease documented with angiography, Diabetes Care 19 (1996) 1–7.

[6] Y. Harano, S. Ohgaku, K. Kosugi, H. Yasuda, T. Nakano, M. Kobayashi, et al., Clinical significance of altered insulin sensitivity in diabetes mellitus assessed by glucose, insulin and somatostatin infusion, J. Clin. Endocrinol. Metab. 52 (1981) 982–987.

[7] M. Suzuki, I. Takamisawa, K. Suzuki, A. Hiuge, T. Horio, Y. Yoshimasa, et al., Close association of endothelial dysfunction with insulin resistance and carotid wall thickening in hypertension, Am. J. Hypertens. 17 (2004) 228–232.

[8] Report of the Expert Committee on the Diagnosis and Classification of Diabetes Mellitus, Diabetes Care 26 (Suppl. 1), 2002, pp. S4–S19.

[9] D.S. Celermajer, K.E. Sorensen, V.M. Gooch, D.J. Spiegelhalter, O.I. Miller, I.D. Sullivan, et al., Non-invasive detection of endothelial dysfunction in children and adults at risk of atherosclerosis, Lancet 340 (1992) 1111–1115.

[10] R. Joannides, W.E. Haefeli, L. Linder, V. Richard, E.H. Bakkali, C. Thuillez, et al., Nitric oxide is responsible for flow-dependent dilatation of human peripheral conduit arteries in vivo, Circulation 91 (1995) 1314–1319.

[11] M. Ikebuchi, M. Suzuki, A. Kageyama, J. Hirose, C. Yokota, K. Ikeda, et al., Modified method using a somatostatin analogue, octreotide acetate (Sandostatin®) to assess in vivo insulin sensitivity, Endocr. J. 43 (1996) 125–130.

[12] B.M. Balletshofer, K. Rittig, M.D. Enderle, A. Volk, E. Maerker, S. Jacob, et al., Endothelial dysfunction is detectable in young normotensive first-degree relatives of subjects with type 2 diabetes in association with insulin resistance, Circulation 101 (2000) 1780–1784.

[13] C. Cardillo, S.S. Nambi, C.M. Kilcoyne, W.K. Choucair, A. Katz, M.J. Quon, et al., Insulin stimulates both endothelin and nitric oxide activity in the human forearm, Circulation 100 (1999) 820–825.

[14] W.A. Hsueh, R.E. Law, 1999 Insulin signaling in the arterial wall, Am. J. Cardiol. 84 (1999) 21J–24J.

[15] G. Zeng, F.H. Nystrom, L.V. Ravichandran, Li-Na. Cong, M. Kirby, H. Mostowski, et al., Roles for insulin receptor, PI3-kinase, and Akt in insulin-signaling pathways related to production of nitric oxide in human vascular endothelial cells, Circulation 101 (2000) 1539–1545.

[16] P.R. Shepherd, D.J. Withers, K. Siddle, Phosphatidylinositol 3-kinase: the key switch mechanism in insulin signaling, Biochem. J. 333 (1998) 471–490.

[17] W. Bagg, G.A. Whalley, G. Gamble, P.L. Drury, N. Sharpe, G.D. Braatvedt, Effects of improved glycaemic control on endothelial function in patients with type 2 diabetes, Intern. Med. J. 31 (2001) 322–328.

[18] K.J. Mather, S. Verma, T.J. Anderson, Improved endothelial function with metformin in type 2 diabetes mellitus, J. Am. Coll. Cardiol. 37 (2001) 1344–1350.
[19] E. Karatzis, J. Lekakis, C. Papamichael, I. Andreadou, A. Cimponeriu, K. Aznaouridis, et al., Rapid effect of pravastatin on endothelial function and lipid peroxidation in unstable angina, Int. J. Cardiol. 101 (2005) 65–70.
[20] P. van der Harst, L.J. Wagenaar, H. Buikema, A.A. Voors, H.W. Plokker, W.J. Morshuis, et al., Effect of intensive versus moderate lipid lowering on endothelial function and vascular responsiveness to angiotensin II in stable coronary artery disease, Am. J. Cardiol. 96 (2005) 1361–1364.
[21] L.O. Jensen, P. Thayssen, K.E. Pedersen, T. Haghfelt, Short- and long-term influence of diet and sinvastatin on brachial artery endothelial function, Int. J. Cardiol. 107 (2006) 101–106.
[22] E. Corrado, I. Muratori, R. Tantillo, F. Contrno, G. Coppola, A. Strano, et al., Relationship between endothelial dysfunction, intima media thickness and cardiovascular risk factors in asymptomatic subjects, Int. Angiol. 24 (2005) 52–58.
[23] K. Noma, C. Goto, K. Nishioka, K. Hara, M. Kimura, T. Umemura, et al., Endothelial function, and Rho-kinase in humans, Arterioscler. Thromb. Vasc. Biol. 25 (2005) 2630–2635.
[24] X.L. Du, D. Edelstein, S. Dimmeler, Q. Ju, C. Sui, M. Brownlee, Hyperglycemia inhibits endothelial nitric oxide synthase activity by posttranslational modification at the Akt site, J. Clin. Invest. 108 (2001) 1341–1348.
[25] H. Kawano, T. Motoyama, O. Hirashima, N. Hirai, Y. Miyao, T. Sakamoto, et al., Hyperglycemia rapidly suppresses flow-mediated endothelium-dependent vasodilation of brachial artery, J. Am. Coll. Cardiol. 31 (1999) 146–154.
[26] F. Pistrosch, K. Fuecker, J. Passauer, M. Hanefeld, S. Fischer, P. Gross, In type 2 diabetes, rosiglitazone therapy for insulin resistance ameliorates endothelial dysfunction independent of glucose control, Diabetes Care 27 (2004) 484–490.

Cardiovascular Research (2008) 80, 339–345
doi:10.1093/cvr/cvn228

Adrenomedullin induces lymphangiogenesis and ameliorates secondary lymphoedema

DongHao Jin[1], Kazuhiko Harada[2], Shunsuke Ohnishi[1], Kenich Yamahara[1], Kenji Kangawa[2], and Noritoshi Nagaya[1]*

[1]*Department of Regenerative Medicine and Tissue Engineering, National Cardiovascular Center Research Institute, 5-7-1 Fujishirodai, Suita, Osaka 565-8565, Japan; and* [2]*Department of Biochemistry, National Cardiovascular Center Research Institute, Osaka, Japan*

Received 8 April 2008; revised 7 August 2008; accepted 11 August 2008; online publish-ahead-of-print 16 August 2008

Time for primary review: 13 days

KEYWORDS
Adrenomedullin;
Lymphangiogenesis;
Lymphoedema

Aims Adrenomedullin (AM) is a multifunctional peptide hormone that plays a significant role in vasodilation and angiogenesis. Lymphoedema is a common but refractory disorder that is difficult to be treated with conventional therapy. We therefore investigated whether AM promotes lymphangiogenesis and improves lymphoedema.

Methods and results The effects of AM on lymphatic endothelial cells (LEC) were investigated. AM promoted proliferation, migration, and network formation of cultured human lymphatic microvascular endothelial cells (HLMVEC). AM increased intracellular cyclic adenosine monophosphate (cAMP) level in HLMVEC. The cell proliferation induced by AM was inhibited by a cAMP antagonist and mitogen-activated protein kinase kinase (MEK) inhibitors. Phosphorylated extracellular signal-regulated kinase (ERK) in HLMVEC was increased by AM. Continuous administration of AM (0.05 μg/kg/min) to BALB/c mice with tail lymphoedema resulted in a decrease in lymphoedema thickness. AM treatment increased the number of lymphatic vessels and blood vessels in the injury site.

Conclusion AM promoted LEC proliferation at least in part through the cAMP/MEK/ERK pathway, and infusion of AM induced lymphangiogenesis and improved lymphoedema in mice.

1. Introduction

Lymphatic system plays an important role in the maintenance of tissue fluid homeostasis,[1] and damage of lymphatic vessels or surgical removal of lymph nodes often triggers the development of lymphoedema.[2,3] Despite substantial advances in surgical and conservative techniques, the therapeutic options for this disease are limited.[4,5] Recently, studies have suggested that vascular endothelial growth factor (VEGF)-C, VEGF-D or hepatocyte growth factor stimulates lymphangiogenesis and promotes oedema recovery in animal models of lymphoedema. The proliferation and migration of lymphatic endothelial cells (LEC) induced by these factors are dependent on activation of extracellular signal-regulated kinase (ERK) and Akt.[6–9]

Adrenomedullin (AM) is a vasodilator and diuretic peptide that was originally isolated from pheochromocytoma cells.[10,11] Earlier studies have shown that AM has protective effects on the cardiovascular system.[12–14] In particular, AM has angiogenic properties through activation of ERK and Akt in vascular endothelial cells.[15–17] Interestingly, a recent study has shown that the AM peptide is widely expressed in breast cancer and the degree of expression is associated with axillary lymph node metastasis.[18] Endogenous AM is necessary for murine lymphatic vascular development during embryogenesis.[19] These findings raise the possibility that AM may play an important role in lymphangiogenesis. However, whether AM promotes lymphangiogenesis and improves lymphoedema remains unknown.

Therefore, the present study was performed to (i) investigate whether AM promotes proliferation, migration, and network formation of cultured LEC *in vitro*, and elucidate the underlying molecular mechanisms and (ii) investigate whether AM promotes lymphangiogenesis and improves lymphoedema in a mouse model of tail lymphoedema *in vivo*.

2. Methods

2.1 Cell culture

Human umbilical vein endothelial cells (HUVEC) and human lymphatic microvascular endothelial cells (HLMVEC) were purchased from Lonza (Basel, Switzerland), and expanded in medium (EBM-2, Lonza) with growth supplements (EGM-2MV, SingleQuots, Lonza). HUVEC and HLMVEC were cultured on collagen I-coated dishes

* Corresponding author. Tel: +81 6 6833 5012; fax: +81 6 6835 5496.
E-mail address: nnagaya@hotmail.co.jp

(Iwaki, Chiba, Japan) and uncoated dishes, respectively. All the cells were used within passages 5–8.

2.2 Characterization of cultured lymphatic endothelial cells

To confirm the purity of expanded HLMVEC, we stained these cells with a LEC-specific marker Prox1.[20] The cells were stained with anti-Prox1 antibody (Acris, Hiddenhausen, Germany) followed by Alexa Fluor 488-conjugated secondary antibody (Invitrogen, Carlsbad, CA, USA), and counterstained with 4',6-diamidino-2-phenylindole (Dojindo, Kumamoto, Japan). The images were obtained with a fluorescence microscope (BZ-9000, Keyence, Osaka, Japan).

To examine the expression of AM receptor messenger ribonucleic acid (mRNA) in HLMVEC, reverse transcription polymerase chain reaction (RT-PCR) was performed. Total RNA were prepared from cultured HLMVEC using an RNeasy mini kit (Qiagen, Hilden, Germany). PCR was carried out on a thermocycler (ASTEC PC-818, Fukuoka, Japan) using the following protocol: an initial denaturation step at 95 C for 5 min, followed by 40 cycles at 95 C for 60 s, 60 C for 30 s, and 72 C for 60 s. The specific primer pairs were: calcitonin-receptor-like receptor (CRLR), 5'-CTCCTCTACATTATCC ATGG-3', and 5'-CCTCCTCTGCAATCTTTCC-3'; receptor-activity-modifying proteins (RAMP) 1, 5'-AGTTCCAGGTAGACATGG-3' and 5'-GCCTACACAATGCCCTCA-3'; RAMP2 5'-AAAGGATTGGTGCGACTG-3' and 5'-GGAAGTGGAGTAACATGG-3'; RAMP3 5'-AGACAGGCATGTT GGAGA-3' and 5'-TTCCAGCTTGCCAGGTGT-3'.[21] A set of β-actin primers was used as a Control for the RT-PCR.

2.3 Cell proliferation assay

HLMVEC were cultured for 36 h in EBM-2 medium containing 5% foetal bovine serum (FBS, Invitrogen) with (10^{-7} M) or without AM (Sionogi, Osaka, Japan). The cells were stained with Diff-Quik (Sysmex Internal Reagents, Kobe, Japan), photographed (BZ-9000, Keyence), and the number of cells was counted. In addition, HLMVEC were cultured in 96-well plates (5000 cells/well) with AM (10^{-9}–10^{-7} M) or 3', 5'-cyclic adenosine monophosphate 8-bromo sodium salt (8-Br-cAMP) (10^{-6}–10^{-4} M) (Calbiochem, San Diego, CA, USA), a cell-permeable cAMP analogue, and cell proliferation were measured by MTS [3-(4,5-dimethylthiazol-2yl)-5-(3-carboxymethoxyphenyl)-2-(4-sulphophenyl)-2H-tetrazolium] assay (Promega, Madison, WI, USA). The reagent was added and plates were incubated for 4 h, and absorbance was measured at 490 nm (Bio-Rad, Hercules, CA, USA).

2.4 Cell migration and network formation assay

Migration assay was performed using a Transwell permeable support (Corning, NY, USA) containing a membranous insert (6.4 mm diameter, pore size 8.0 μm, collagen matrix uncoated). HLMVEC in EBM-2 with 5% FBS were added to the upper chamber at a density of 10^5 cells/cm^2, AM (10^{-9}–10^{-7} M) in EBM-2 medium containing 5% FBS was added to both the lower and upper chambers or to the lower chamber only, and HLMVECs were allowed to migrate for 12 h at 37 C. The cells remaining at the upper surface of the membrane were scraped off, and the cells on the lower side of the membrane were stained with Diff-Quik (Sysmex Internal Reagents), then the number of migrated cells was counted under a microscope (BZ-9000, Keyence).

Network formation assay was performed using Matrigel tissue culture plates (12-well plates, Becton Dickinson, San Jose, CA, USA). HLMVEC (10^5 cells/well) were seeded into each well and incubated for 18 h in EBM-2 medium containing 5% FBS with (10^{-7} M) or without AM. During this period, the morphologic changes of the cells were observed under a microscope (BZ-9000, Keyence).

2.5 Analysis of intracellular signalling

Intracellular cAMP was measured as reported previously.[22] Briefly, following treatment of HLMVEC (2×10^5 cells) with various concentrations of AM for 5 min, the medium was removed and washed twice with PBS (phosphate buffered saline). The cellular extract was obtained by addition of cold 70% ethanol. Each ethanol sample was evaporated in a vacuum until dry and dissolved in radioimmunoassay (RIA) buffer. cAMP was measured using an RIA kit (cAMP assay kit, Yamasa Shoyu, Chiba, Japan). Radioactivity was measured with a gamma counter (Aloka, Tokyo, Japan).

HLMVEC (5000 cells/well in 96-well plates) were pretreated for 30 min with 3', 5'-cyclic adenosine monophosphorothioate Rp-isomer (Rp-cAMP) (10^{-3} M, Calbiochem), an antagonist of cAMP, PD98059, and U0126 (5×10^{-6} and 10^{-6} M, respectively, Calbiochem), inhibitors of mitogen-activated protein kinase kinase (MEK). The cells were further incubated for 36 h with AM (10^{-7} M) or 8-Br-cAMP (10^{-4} M) then MTS assay was performed as described previously.

2.6 Animal model and adrenomedullin administration

Male BALB/c mice (8–10 weeks, Japan SLC, Hamamatsu, Japan) were randomly divided into two groups: an AM treatment group and a Control group ($n = 10$ in each group). Tail lymphoedema was created as described previously with modification.[23] In brief, mice were anaesthetized by intraperitoneal injection of pentobarbital sodium (30 mg/kg, Dainippon Sumitomo Pharma, Osaka, Japan). A 1.5–2 mm-wide ring of skin was removed 1 cm distal to the tail base, leaving the underlying bone, muscle and major blood vessels intact, and then the tail was wrapped with adhesive tape to protect the surgical site from interference. The AM group received continuous subcutaneous injection of recombinant human AM (Shionogi) dissolved in 0.9% saline at a rate of 0.05 μg/kg/min for 14 days from the day of operation, using an osmotic minipump (Alzet, Cupertino, CA, USA).[24,25] The Control group received 0.9% saline instead of AM.

All protocols were performed in accordance with the guidelines of the Animal Care Ethics Committee of the National Cardiovascular Center Research Institute. The investigation conformed to the *Guide for the Care and Use of Laboratory Animals* published by the US National Institutes of Health (NIH Publication No. 85–23, revised 1996).

2.7 Measurements of plasma adrenomedullin concentration and tail lymphoedema

Twenty-four hours after the start of AM administration, blood samples were collected into ice-cooled tubes with 70 μg/mL aprotinin and 1.5 mg/mL ethylenediaminetetraacetic acid 2Na (Bayer, Leverkusen, Germany), immediately centrifuged at 4 C, and stored at −80 C until use. Plasma human AM level was measured using an immunoradiometric assay kit (Shionogi), as described previously.[26] In brief, 200 μL of standard or plasma sample was placed in a polystyrene tube, and a mixture of biotinylated anti-AM and iodolabelled anti-AM was added. One bead coated with anti-biotin antibody was added (total volume = 300 μL), and the mixture was incubated at 4 C for 20 h. After removal of the incubation mixture, the bead was washed twice with 2 mL distilled water and radioactivity was measured with a gamma counter (Aloka).

Two days after operation, the tape wrapping the injury site was removed, and tail diameter at 1 cm distal to the distal edge of the injury site was measured by a calliper. Measurement was performed every other day until the mice were sacrificed on day 16 postoperation.

2.8 Fluorescence microlymphangiography

Lymphatic vessels in the dermis of the tail were evaluated by fluorescence microlymphangiography as previously described.[23] In brief, mice were anaesthetized by intraperitoneal injection of pentobarbital sodium (30 mg/kg) on day 16 postoperation. Fluorescein isothiocyanate (FITC)-dextran (70 kDa, Sigma-Aldrich) (2 mg/mL) was infused into the tip of the mouse tail. Then, images of superficial capillaries of the tail were photographed (MZ16FA, Leica Microsystems, Wetzlar, Germany).

2.9 Immunohistochemical study

On day 16 postoperation, the injury sites were removed, fixed in 4% paraformaldehyde, embedded with paraffin, and cut into 5 μm sections. For antigen retrieval, the sections were incubated with citrate buffer (DAKO, Glostrup, Denmark) at 120 C for 10 min. After treatment with protein block (DAKO), the samples were incubated with anti-lymphatic endothelial hyaluronan receptor-1 (LYVE-1) antibody (R&D Systems, Minneapolis, MN, USA), anti-Podoplanin antibody (Acris) or anti-von Willebrand factor (vWF) antibody (AB7356, Chemicon, Temecula, CA, USA) for 1 h at room temperature, and further incubated with horseradish peroxidase-conjugated antibodies (DAKO), then visualized with a DAB kit (Wako, Osaka, Japan). Cell nuclei were counterstained with haematoxylin (Muto, Tokyo, Japan).

2.10 Western blot analysis

HLMVEC were incubated for 12 h in basal medium containing 5% FBS and stimulated with (10^{-7} M) or without AM, then lysed in sample buffer with protease inhibitor (Complete, Roche, IN, USA). The lysates were loaded on 7.5% sodium dodecylsulphate-polyacrylamide gels (Bio-Rad, Hercules, CA, USA), transferred to membranes (Millipore, MA, USA) and probed with anti-ERK and anti-phosphorylated ERK (p-ERK) (Thr202/Thr204) antibodies (Cell Signaling, Boston, MA, USA) or anti-Akt and anti-phosphorylated Akt (p-Akt) (Ser473) antibodies (Cell Signaling). An anti-β-actin antibody (Sigma-Aldrich, St Louis, MO, USA) served as a loading control. The membranes were then incubated with horseradish peroxidase-conjugated antibodies (Cell Signaling), and visualized by enhanced chemiluminescence reaction (GE Healthcare, Piscataway, NJ, USA).

HLMVEC were stimulated with (10^{-7} M) or without AM for 12 h, then lysed in sample buffer. Tail tissue of the injury site was obtained on day 8 postoperation and also lysed in sample buffer. Concentrations of VEGF-C and VEGF-A in each lysate were measured by western blot analysis. An anti-VEGF-C (H-190, Santa Cruz Biotech, Santa Cruz, CA, USA) antibody or an anti-VEGF-A (VEGF147, Santa Cruz, for HLMVEC lysate; AB1442, Chemicon, for tail tissue lysate) antibody was used as the probe. A rabbit polyclonal antibody against α-tubulin (Abcam, Cambridge, MA, USA) was used as an internal control.

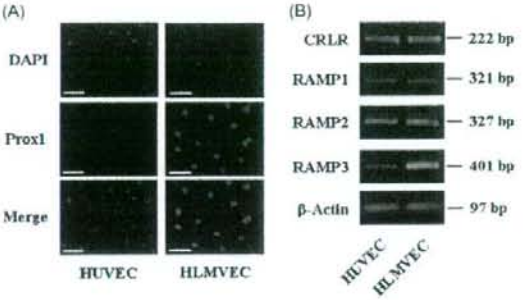

Figure 1 Characteristics of cultured human lymphatic microvascular endothelial cells (HLMVEC). (*A*) Fluorescent images of human umbilical vein endothelial cells (HUVEC) and HLMVEC, stained with anti-Prox1 antibody (green) and 4',6-diamidino-2-phenylindole (blue). Scale bars: 50 μm. All HLMVEC stained positive for Prox1. (*B*) HLMVEC expressed CRLR (calcitonin-receptor-like receptor), RAMP1 (receptor-activity-modifying protein), RAMP2, and RAMP3 mRNA (messenger ribonucleic acid). HUVEC were used as a control.

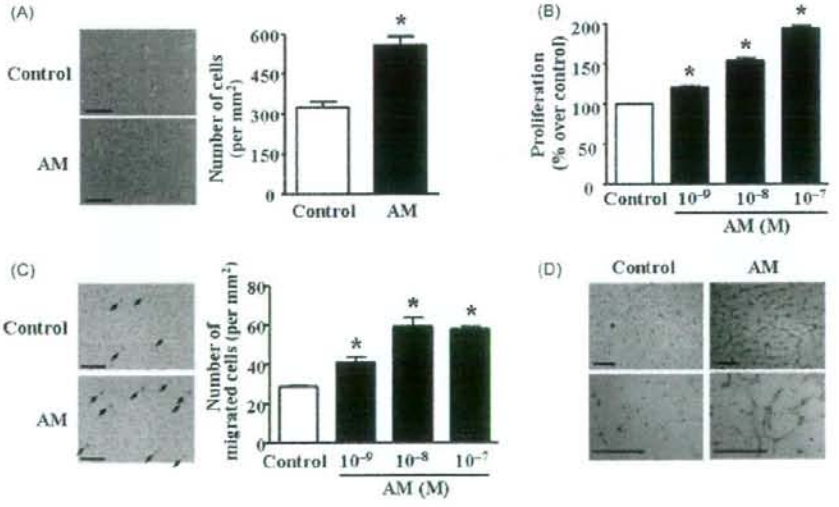

Figure 2 Effects of adrenomedullin (AM) on lymphatic endothelial cells (LEC). (*A*) Left panels, representative photographs of cultured human lymphatic microvascular endothelial cells (HLMVEC), stimulated with AM (10^{-7} M) for 36 h and stained with Diff-Quik. Scale bars: 200 μm. Right panel, quantitative analysis of proliferated HLMVEC ($n = 4$). (*B*) MTS [3-(4,5-dimethylthiazol-2yl)-5-(3-carboxymethoxyphenyl)-2-(4-sulphophenyl)-2H-tetrazolium] assay demonstrated dose-dependent promotion of proliferation in cultured HLMVEC by AM ($n = 8$). (*C*) Left panels, representative photographs of HLMVEC in migration assay, stimulated with AM (10^{-7} M) for 12 h and stained with Diff-Quik. Arrows indicate migrated cells. Scale bars: 100 μm. Right panel, quantitative analysis of migrated cells ($n = 6$). (*D*) Representative photographs of HLMVEC in network formation assay, stimulated with AM (10^{-7} M) for 18 h. Scale bars: 500 μm. Data are mean ± SE. *$P < 0.05$ vs. Control.

2.11 Statistical analysis

All data are expressed as mean ± SE. Comparisons of parameters among the groups were made by one-way ANOVA (analysis of variance), followed by Newman-Keul's test. Comparisons of parameters between two groups were made by Student's *t*-test. Values of $P < 0.05$ were considered statistically significant.

3. Results

3.1 Expression of calcitonin-receptor-like receptor and receptor-activity-modifying proteins mRNA in lymphatic endothelial cells

To determine whether LEC express AM receptors, we analysed commercially available HLMVEC which were positive for lymphatic maker Prox1 (*Figure 1A*). HLMVEC expressed CRLR, RAMP1, RAMP2, and RAMP3 mRNA (*Figure 1B*).

3.2 Enhancement of proliferation, migration, and network formation in cultured lymphatic endothelial cells by adrenomedullin

AM (10^{-7} M) significantly increased the number of cultured HLMVEC (*Figure 2A*). MTS assay also demonstrated that AM enhanced proliferation of cultured HLMVEC in a dose-dependent manner (*Figure 2B*). The number of migrated cells was significantly increased by AM (10^{-9}–10^{-7} M) when it was added to the lower chamber only (*Figure 2C*). This result indicates that AM is chemotactic for LEC. In addition, a marked increase in network formation was observed in the AM (10^{-7} M) group as compared with the Control group (*Figure 2D*). These results suggest that AM promotes proliferation, migration, and network formation of LEC.

3.3 Activation of cAMP/MEK/ERK pathway in lymphatic endothelial cells by adrenomedullin

We examined whether AM increases intracellular cAMP, the major second messenger of AM,[27,28] in cultured HLMVEC. AM dose-dependently increased the cAMP level in these cells (*Figure 3A*). Cell proliferation induced by AM was inhibited by a cAMP antagonist, Rp-cAMP (*Figure 3B*). In addition, a cAMP analogue, 8-Br-cAMP induced proliferation of HLMVEC in a dose-dependent manner (*Figure 3C*).

ERK and Akt are known to regulate cell proliferation and these signalling pathways were reported to function downstream of the AM/cAMP pathway.[29,30] Therefore, we investigated the activity (phosphorylation) of ERK and Akt in cultured LEC after stimulation with AM. The level of p-ERK in HLMVEC was significantly increased as early as 5 min after the start of AM (10^{-7} M) stimulation (*Figure 4A*). In contrast, the level of p-Akt in HLMVEC was not markedly increased by AM (*Figure 4B*). In addition, the cell proliferation induced by AM or 8-Br-cAMP was significantly attenuated by MEK inhibitors, PD98059, and U0126 (*Figure 4C* and *D*). These results suggest that AM-induced cell proliferation is mediated at least in part by the cAMP/MEK/ERK pathway.

3.4 Improvement of mouse tail lymphoedema by adrenomedullin

To evaluate the effect of AM on lymphoedema, a mouse model of tail lymphoedema was developed in BALB/c mice, and human AM was administered to the mice at a rate of 0.05 μg/kg/min (*Figure 5A*). Plasma human AM level was 5.4 ± 0.9 fM in AM-treated mice, whereas human AM was not detected in Control mice. The tail became oedematous after the surgical procedure and this change peaked on day 8 postoperation then gradually recovered in the AM and Control groups. However, AM treatment promoted the recovery of the injury site (*Figure 5B*). A significant difference in tail thickness was observed on days 14 and 16 postoperation (*Figure 5C*). These results suggest that AM improves secondary lymphoedema of the tail in mice.

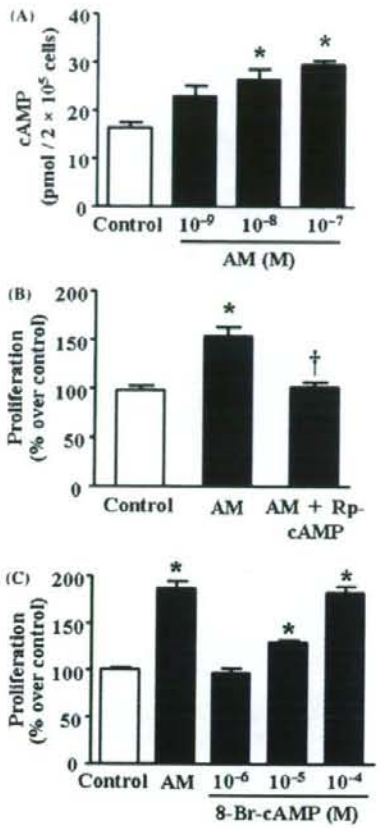

Figure 3 Relation between adrenomedullin (AM) and cyclic adenosine monophosphate (cAMP) in lymphatic endothelial cells (LEC) proliferation. (*A*) Following stimulation of human lymphatic microvascular endothelial cells (HLMVEC) with AM (10^{-9}–10^{-7} M) for 5 min, cAMP concentration was dose-dependently increased ($n = 4$). (*B*) MTS assay demonstrated that AM (10^{-7} M)-induced proliferation of HLMVEC was inhibited by a cAMP antagonist, Rp-cAMP (10^{-3} M) ($n = 8$). (*C*) MTS [3-(4,5-dimethylthiazol-2yl)-5-(3-carboxymethoxyphenyl)-2-(4-sulphophenyl)-2H-tetrazolium] assay demonstrated that a cAMP analogue, 8-Br-cAMP enhanced the proliferation of cultured HLMVEC in a dose-dependent manner ($n = 8$). Data are mean ± SE. *$P < 0.05$ vs. Control, †$P < 0.05$ vs. AM.

3.5 Promotion of lymphangiogenesis and angiogenesis by adrenomedullin

Lymphatic flow in the tail was evaluated by fluorescence microlymphangiography on day 16 postoperation

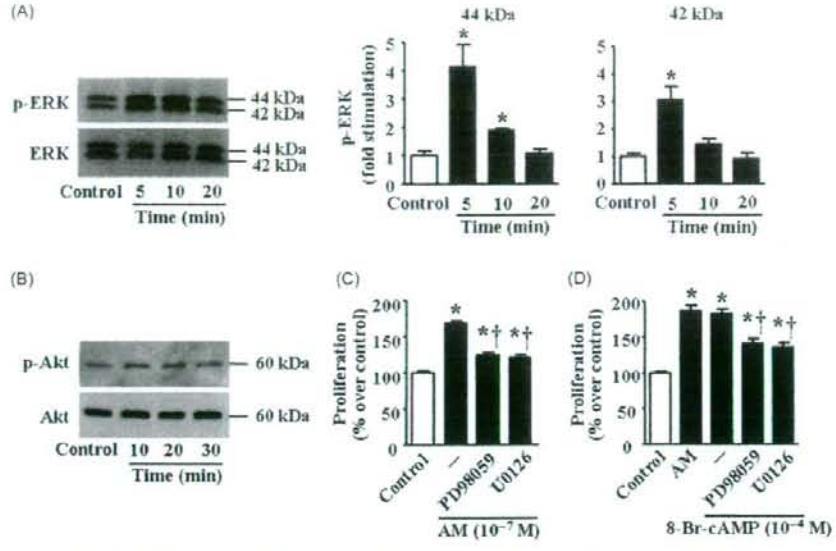

Figure 4 Intracellular signalling pathway induced by adrenomedullin (AM) in lymphatic endothelial cells (LEC). (*A*) Left panels, western blot analysis of phosphorylated extracellular signal-regulated kinase (p-ERK) and ERK in human lymphatic microvascular endothelial cells (HLMVEC), stimulated with AM (10^{-7} M) for 5, 10, and 20 min. Middle and right panel, quantitative analysis of p-ERK (44 and 42 kDa) ($n = 4$). (*B*) Western blot analysis of phosphorylated Akt (p-Akt) and Akt in HLMVEC, stimulated with AM (10^{-7} M) for 10, 20, and 30 min. (*C* and *D*) AM (10^{-7} M) or 8-Br-cAMP (cyclic adenosine monophosphate) (10^{-4} M)-induced proliferation of HLMVEC was inhibited by mitogen-activated protein kinase kinase (MEK) inhibitors, PD98059 and U0126 ($n = 6$). Data are mean ± SE. $^{*}P < 0.05$ vs. Control, $^{\dagger}P < 0.05$ vs. AM or 8-Br-cAMP.

(*Figure 6A*). After infusion of FITC-dextran, fluorescence was soon observed in the distal part of the injury site. Although slow drainage of FITC-dextran was seen in Control group, rapid movement of fluorescence to the proximal part of the injury site was observed in the AM group.

Lymphatic vessels in the injury site were revealed by staining with anti-LYVE-1 antibody or anti-Podoplanin antibody. Blood vessels in the injury site were visualized by staining with anti-vWF antibody (*Figure 6B*). A large number of LYVE-1-, Podoplanin-, and vWF-positive vessels were observed on day 16 postoperation. The density of lymphatic vessels and blood vessels in the injury site was higher in the AM group than in the Control group. We determined the expression of VEGF-C and VEGF-A in the injury site after AM administration. Western blot analysis demonstrated that expression of VEGF-C or VEGF-A was not notably affected by AM (0.05 μg/kg/min) administration. *In vitro* study also demonstrated that the expression of VEGF-C or VEGF-A in HLMVEC was not significantly changed by AM (10^{-7} M) stimulation. These results suggest that AM directly promotes lymphangiogenesis and angiogenesis in a mouse model of tail lymphoedema.

4. Discussion

In this study, we demonstrated that (i) AM augmented proliferation and migration of LEC, and that the proliferation induced by AM was mediated at least in part by the cAMP/MEK/ERK pathway and (ii) administration of AM promoted lymphangiogenesis and improved mouse secondary lymphoedema.

AM has a variety of biological effects including angiogenic properties.[31–33] However, whether AM induces lymphangiogenesis and what is the underling mechanism responsible for the process remain unknown. In the present study, HLMVEC expressed CRLR, RAMP1, RAMP2, and RAMP3 mRNA. This suggests that AM could stimulate LEC through a complex of CRLR and one of the three RAMPs. Treatment of cultured HLMVEC with AM enhanced cell proliferation. Migration assay and network formation assay also demonstrated that AM enhanced cell migration and network formation. The process of lymphangiogenesis is known to include proliferation and migration of LEC,[9,34] therefore, AM-induced lymphangiogenesis is mediated by promotion of proliferation and migration of LEC.

Earlier studies have shown that cAMP plays an important role in proliferation of vascular endothelial cells.[35] In the present study, AM increased intracellular cAMP level in HLMVEC, and the proliferation induced by AM was inhibited by a cAMP antagonist Rp-cAMP. ERK in cultured LEC was markedly activated by treatment with AM. In addition, AM- or 8-Br-cAMP-induced cell proliferation was attenuated by MEK inhibitors, PD98069 and U0126. These results suggest that AM-induced cell proliferation is mediated by cAMP and at least in part through its downstream MEK/ERK pathway. In fact, cAMP-dependent ERK activation has been shown in the proliferation of HUVEC following adenosine receptor stimulation.[36]

We demonstrated the therapeutic potential of AM for lymphoedema using a mouse model of tail lymphoedema. The mouse tail exhibits a highly regular hexagonal network of lymphatic vessels in the skin. Therefore, depletion of circumferential skin in the tail obstructs lymphatic flow, resulting in acute lymphoedema, so this system could serve as a model of secondary lymphoedema to examine lymphangiogenesis *in vivo*.[7,23] Mature AM peptide consists of 52

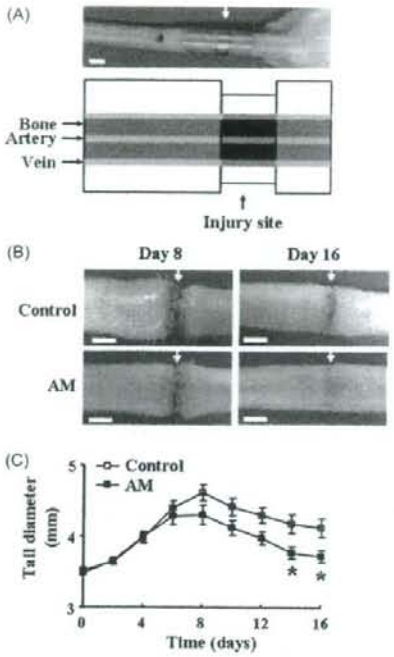

Figure 5 Effect of adrenomedullin (AM) infusion on mouse tail lymphoedema. (A) Upper panel, an operative model of mouse tail lymphoedema was created by removing tail skin circumferentially 1 cm distal to the tail base. Arrow indicates injury site. Scale bar: 2 mm. Lower panel, schematic diagram of injury site. (B) Representative photographs of tail on days 8 and 16 postoperation. Arrows indicate injury sites. Scale bars: 2 mm. (C) Quantitative analysis demonstrated a significant decrease in tail thickness in AM-treated mice vs. Control mice on days 14 and 16 postoperation ($n = 10$). Data are mean ± SE. $^*P < 0.05$ vs. Control.

amino acids in humans and 50 amino acids in the mouse. Mouse AM is 88% identical to human AM.[37,38] Administration of human AM to the mouse exerts biological effects *in vivo*.[32,39] In the present study, continuous administration of human recombinant AM at a rate of 0.05 μg/kg/min promoted recovery of the injury site and promoted a decrease in tail thickness. The number of LYVE-1- or Podoplanin-positive lymphatic vessels and vWF-positive blood vessels in the injury site were significantly increased in AM-treated mice. These findings suggest that AM improves lymphoedema and induces both lymphangiogenesis and angiogenesis. The mechanism of accelerated healing of the tail injury in AM-treated mice is unclear. However, previous studies showed that angiogenesis as well as lymphangiogenesis is crucial in the wound-healing process.[40,41] Therefore, the accelerated healing of the tail injury may be explained in part by increased blood vessels and lymphatic vessels in AM-treated mice.

VEGF-C and VEGF-A are key factors in lymphangiogenesis and angiogenesis.[42,43] However, in the present study, AM did not affect the expression of VEGF-C or VEGF-A in the tail tissue or in cultured HLMVEC. These results suggest that AM may directly stimulate LEC and endothelial cells to promote lymphangiogenesis and angiogenesis in our animal model.

In conclusion, AM promoted LEC proliferation at least in part through the cAMP/MEK/ERK pathway. Administration of AM improved secondary lymphoedema, and promoted lymphangiogenesis and angiogenesis. Thus, administration of AM may be a novel therapeutic strategy for patient with lymphoedema.

Funding

Funding for this work was provided by research grants for Cardiovascular Disease (19C-7, 17A-1) from the Ministry of Health, Labour and Welfare; the Program for Promotion of Fundamental Studies in Health Sciences of the National Institute of Biomedical Innovation (NIBIO);

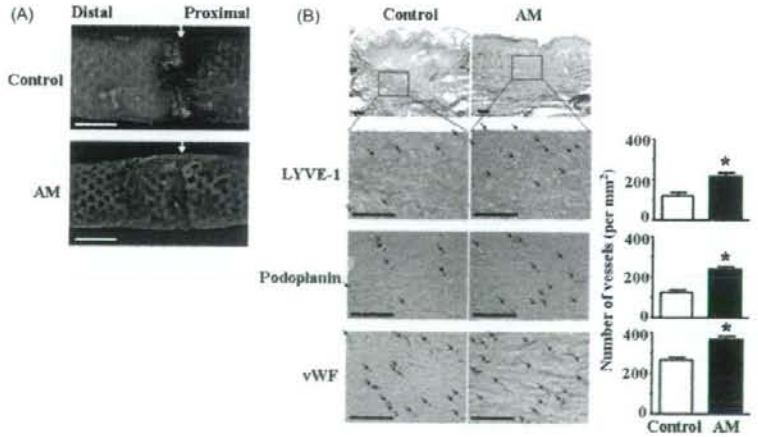

Figure 6 Histological analysis of lymphangiogenesis and angiogenesis. (A) Representative photographs of lymphatic flow in mouse tail. Fluorescence was mainly observed in the distal part of the injury site in Control mice, but was observed in the whole area of the tail in adrenomedullin (AM)-treated mice. Arrows indicate injury sites. Scale bars: 2 mm. (B) Left panels, representative photographs of tail sections on day 16 postoperation, immunostained with anti-LYVE-1 (lymphatic endothelial hyaluronan receptor-1), anti-Podoplanin and anti-vWF (von Willebrand factor) antibodies. Arrows indicate LYVE-1-, Podoplanin- or vWF-positive vessels. Left upper panels show the whole area of the injury site. Scale bars: 100 μm. Right panels, quantitative analysis demonstrated significant increases in LYVE-1- and Podoplanin-positive lymphatic vessels, and vWF-positive blood vessels in AM-treated mice vs. Control mice ($n = 5$). Data are mean ± SE. $^*P < 0.05$ vs. Control.

the Takeda Scientific Foundation; and the Japan Vascular Disease Research Foundation.

Conflict of interest: none declared.

References

1. Adams RH, Alitalo K. Molecular regulation of angiogenesis and lymphangiogenesis. *Nat Rev Mol Cell Biol* 2007;**8**:464-478.
2. Alitalo K, Tammela T, Petrova TV. Lymphangiogenesis in development and human disease. *Nature* 2005;**438**:946-953.
3. Szuba A, Rockson SG. Lymphedema: anatomy, physiology and pathogenesis. *Vasc Med* 1997;**2**:321-326.
4. Mortimer PS. Therapy approaches for lymphedema. *Angiology* 1997;**48**: 87-91.
5. Kligman L, Wong RK, Johnston M, Laetsch NS. The treatment of lymphedema related to breast cancer: a systematic review and evidence summary. *Support Care Cancer* 2004;**12**:421-431.
6. Oh SJ, Jeltsch MM, Birkenhager R, McCarthy JE, Weich HA, Christ B *et al.* VEGF and VEGF-C: specific induction of angiogenesis and lymphangiogenesis in the differentiated avian chorioallantoic membrane. *Dev Biol* 1997; **188**:96-109.
7. Saito Y, Nakagami H, Morishita R, Takami Y, Kikuchi Y, Hayashi H *et al.* Transfection of human hepatocyte growth factor gene ameliorates secondary lymphedema via promotion of lymphangiogenesis. *Circulation* 2006;**114**:1177-1184.
8. Szuba A, Skobe M, Karkkainen MJ, Shin WS, Beynet DP, Rockson NB *et al.* Therapeutic lymphangiogenesis with human recombinant VEGF-C. *FASEB J* 2002;**16**:1985-1987.
9. Makinen T, Veikkola T, Mustjoki S, Karpanen T, Catimel B, Nice EC *et al.* Isolated lymphatic endothelial cells transduce growth, survival and migratory signals via the VEGF-C/D receptor VEGFR-3. *EMBO J* 2001;**20**:4762-4773.
10. Nuki C, Kawasaki H, Kitamura K, Takenaga M, Kangawa K, Eto T *et al.* Vasodilator effect of adrenomedullin and calcitonin gene-related peptide receptors in rat mesenteric vascular beds. *Biochem Biophys Res Commun* 1993;**196**:245-251.
11. Jougasaki M, Wei CM, Aarhus LL, Heublein DM, Sandberg SM, Burnett JC Jr. Renal localization and actions of adrenomedullin: a natriuretic peptide. *Am J Physiol* 1995;**268**:F657-F663.
12. Kato J, Kitamura K, Eto T. Plasma adrenomedullin level and development of hypertension. *J Hum Hypertens* 2006;**20**:566-570.
13. Nakamura R, Kato J, Kitamura K, Onitsuka H, Imamura T, Cao Y *et al.* Adrenomedullin administration immediately after myocardial infarction ameliorates progression of heart failure in rats. *Circulation* 2004;**110**: 426-431.
14. Okumura H, Nagaya N, Itoh T, Okano I, Hino J, Mori K *et al.* Adrenomedullin infusion attenuates myocardial ischemia/reperfusion injury through the phosphatidylinositol 3-kinase/Akt-dependent pathway. *Circulation* 2004;**109**:242-248.
15. Kato J, Tsuruda T, Kita T, Kitamura K, Eto T. Adrenomedullin: a protective factor for blood vessels. *Arterioscler Thromb Vasc Biol* 2005;**25**: 2480-2487.
16. Miyashita K, Itoh H, Sawada N, Fukunaga Y, Sone M, Yamahara K *et al.* Adrenomedullin provokes endothelial Akt activation and promotes vascular regeneration both in vitro and in vivo. *FEBS Lett* 2003;**544**:86-92.
17. Kim W, Moon SO, Sung MJ, Kim SH, Lee S, So JN *et al.* Angiogenic role of adrenomedullin through activation of Akt, mitogen-activated protein kinase, and focal adhesion kinase in endothelial cells. *FASEB J* 2003;**17**: 1937-1939.
18. Oehler MK, Fischer DC, Orlowska-Volk M, Herrle F, Kieback DG, Rees MC *et al.* Tissue and plasma expression of the angiogenic peptide adrenomedullin in breast cancer. *Br J Cancer* 2003;**89**:1927-1933.
19. Fritz-Six KL, Dunworth WP, Li M, Caron KM. Adrenomedullin signaling is necessary for murine lymphatic vascular development. *J Clin Invest* 2008;**118**:40-50.
20. Rodriguez-Niedenfuhr M, Papoutsi M, Christ B, Nicolaides KH, von Kaisenberg CS, Tomarev SI *et al.* Prox1 is a marker of ectodermal placodes, endodermal compartments, lymphatic endothelium and lymphangioblasts. *Anat Embryol (Berl)* 2001;**204**:399-406.
21. Nikitenko LL, Blucher N, Fox SB, Bicknell R, Smith DM, Rees MC. Adrenomedullin and CGRP interact with endogenous calcitonin-receptor-like receptor in endothelial cells and induce its desensitisation by different mechanisms. *J Cell Sci* 2006;**119**:910-922.
22. Nishikimi T, Horio T, Yoshihara F, Nagaya N, Matsuo H, Kangawa K. Effect of adrenomedullin on cAMP and cGMP levels in rat cardiac myocytes and nonmyocytes. *Eur J Pharmacol* 1998;**353**:337-344.
23. Boardman KC, Swartz MA. Interstitial flow as a guide for lymphangiogenesis. *Circ Res* 2003;**92**:801-808.
24. Nagaya N, Satoh T, Nishikimi T, Uematsu M, Furuichi S, Sakamaki F *et al.* Hemodynamic, renal, and hormonal effects of adrenomedullin infusion in patients with congestive heart failure. *Circulation* 2000;**101**:498-503.
25. Nagaya N, Nishikimi T, Horio T, Yoshihara F, Kanazawa A, Matsuo H *et al.* Cardiovascular and renal effects of adrenomedullin in rats with heart failure. *Am J Physiol* 1999;**276**:R213-R218.
26. Nagaya N, Kyotani S, Uematsu M, Ueno K, Oya H, Nakanishi N *et al.* Effects of adrenomedullin inhalation on hemodynamics and exercise capacity in patients with idiopathic pulmonary arterial hypertension. *Circulation* 2004;**109**:351-356.
27. Kato J, Kitamura K, Kangawa K, Eto T. Receptors for adrenomedullin in human vascular endothelial cells. *Eur J Pharmacol* 1995;**289**:383-385.
28. Shimekake Y, Nagata K, Ohta S, Kambayashi Y, Teraoka H, Kitamura K *et al.* Adrenomedullin stimulates two signal transduction pathways, cAMP accumulation and Ca^{2+} mobilization, in bovine aortic endothelial cells. *J Biol Chem* 1995;**270**:4412-4417.
29. Yu Y, Sato JD. MAP kinases, phosphatidylinositol 3-kinase, and p70 S6 kinase mediate the mitogenic response of human endothelial cells to vascular endothelial growth factor. *J Cell Physiol* 1999;**178**:235-246.
30. Ilan N, Mahooti S, Madri JA. Distinct signal transduction pathways are utilized during the tube formation and survival phases of in vitro angiogenesis. *J Cell Sci* 1998;**111**:3621-3631.
31. Nagaya N, Mori H, Murakami S, Kangawa K, Kitamura S. Adrenomedullin: angiogenesis and gene therapy. *Am J Physiol Regul Integr Comp Physiol* 2005;**288**:R1432-R1437.
32. Iimuro S, Shindo T, Moriyama N, Amaki T, Niu P, Takeda N *et al.* Angiogenic effects of adrenomedullin in ischemia and tumor growth. *Circ Res* 2004; **95**:415-423.
33. Tokunaga N, Nagaya N, Shirai M, Tanaka E, Ishibashi-Ueda H, Harada-Shiba M *et al.* Adrenomedullin gene transfer induces therapeutic angiogenesis in a rabbit model of chronic hind limb ischemia: benefits of a novel nonviral vector, gelatin. *Circulation* 2004;**109**:526-531.
34. Rutkowski JM, Boardman KC, Swartz MA. Characterization of lymphangiogenesis in a model of adult skin regeneration. *Am J Physiol Heart Circ Physiol* 2006;**291**:H1402-H1410.
35. Meininger CJ, Granger HJ. Mechanisms leading to adenosine-stimulated proliferation of microvascular endothelial cells. *Am J Physiol* 1990;**258**: H198-H206.
36. Fang Y, Olah ME. Cyclic AMP-dependent, protein kinase A-independent activation of extracellular signal-regulated kinase 1/2 following adenosine receptor stimulation in human umbilical vein endothelial cells: role of exchange protein activated by cAMP 1 (Epac1). *J Pharmacol Exp Ther* 2007;**322**:1189-1200.
37. Kitamura K, Sakata J, Kangawa K, Kojima M, Matsuo H, Eto T. Cloning and characterization of cDNA encoding a precursor for human adrenomedullin. *Biochem Biophys Res Commun* 1993;**194**:720-725.
38. Okazaki T, Ogawa Y, Tamura N, Mori K, Isse N, Aoki T *et al.* Genomic organization, expression, and chromosomal mapping of the mouse adrenomedullin gene. *Genomics* 1996;**37**:395-399.
39. Ashton D, Hieble P, Gout B, Alyar N. Vasodilatory effect of adrenomedullin in mouse aorta. *Pharmacology* 2000;**61**:101-105.
40. Tonnesen MG, Feng X, Clark RA. Angiogenesis in wound healing. *J Investig Dermatol Symp Proc* 2000;**5**:40-46.
41. Hirakawa S, Detmar M. New insights into the biology and pathology of the cutaneous lymphatic system. *J Dermatol Sci* 2004;**35**:1-8.
42. Jeltsch M, Kaipainen A, Joukov V, Meng X, Lakso M, Rauvala H *et al.* Hyperplasia of lymphatic vessels in VEGF-C transgenic mice. *Science* 1997;**276**:1423-1425.
43. Cao R, Eriksson A, Kubo H, Alitalo K, Cao Y, Thyberg J. Comparative evaluation of FGF-2-, VEGF-A-, and VEGF-C-induced giogenesis, lymphangiogenesis, vascular fenestrations, and permeability. *Circ Res* 2004;**94**: 664-670.

Journal of Cellular Physiology

Highly Efficient and Feeder-Free Production of Subculturable Vascular Endothelial Cells From Primate Embryonic Stem Cells

KUMIKO SAEKI,[1] YOSHIKO YOGIASHI,[1] MASAKO NAKAHARA,[1] NAOKO NAKAMURA,[1] SATOKO MATSUYAMA,[1] AKEMI KOYANAGI,[2] HIDEO YAGITA,[2] MAKOTO KOYANAGI,[1] YASUSHI KONDO,[3] AND AKIRA YUO[1]*

[1]*Department of Hematology, Research Institute, International Medical Center of Japan, Tokyo, Japan*

[2]*Department of Immunology, Juntendo University School of Medicine, Tokyo, Japan*

[3]*Regenerative Medicine Group, Advanced Medical Research Laboratory, Mitsubishi Tanabe Pharma Corporation, Osaka, Japan*

The vascular endothelial cell (VEC) differentiation from primate embryonic stem (ES) cells has critical problems: low differentiation efficiencies (<2%) and/or subculture incapability. We report a novel feeder-free culture method for high efficiency production of subculturable VECs from cynomolgus monkey ES cells. Spheres, which were generated from ES cells in the presence of cytokine cocktail, were cultured on gelatin-coated plates. Cobblestone-shaped cells spread out after a few days, which were followed by an emergence of a sac-like structure containing hematopoietic cells. All adherent cells including sac walls cells and surrounding cobblestone cells expressed vascular endothelial cadherin (VE-cadherin) at intercellular junctions. Subculture of these cells resulted in a generation of homogeneous spindle-shaped population bearing cord-forming activities and a uniform acetylated low density lipoprotein-uptaking capacity with von Willbrand factor and endothelial nitric oxide synthetase expressions. They were freeze–thaw-tolerable and subculturable up to eight passages. Co-existence of pericytes or immature ES cells was ruled out. When introduced in a collagen sponge plug implanted intraperitoneally in mice, ES-derived cells recruited into neovascularity. Although percentages of surface VE-cadherin-positive population varied from 20% to 80% as assessed by flow cytometry, the surface VE-cadherin-negative population showed intracellular VE-cadherin expression and mature functions, as we call it as atypical VECs. When sorted, the surface VE-cadherin-positive population expanded as almost pure (>90%) VE-cadherin/PECAM-1-positive VECs by 160-fold after five passages. Thus, our system provides pure production of functional, subculturable and freeze–thaw-tolerable VECs, including atypical VECs, from primate ES cells.

J. Cell. Physiol. 217: 261–280, 2008.

Embryonic stem (ES) cells are a valuable resource in regenerative medicine because of their high capacity to differentiate into a broad range of cell types. It has been revealed that primate ES cells have characteristics distinct from those of murine ES cells. For example, leukemia inhibitory factor is ineffective for maintaining the immaturity of human ES cells (Sato et al., 2004). The gene expression patterns also differ between primate and murine ES cells. For example, undifferentiated primate ES cells express kinase insert domain receptor (KDR, Flk-1, a type 2 receptor for vascular endothelial growth factor (VEGF-R2)) although undifferentiated murine ES cells do not (Sone et al., 2003; Vodyanik et al., 2005). KDR is known as an excellent marker for sorting the vascular endothelial precursor population in murine ES differentiation system (Yamashita et al., 2000). However, the presence of KDR in undifferentiated primate ES cells limits a direct application of the murine system to the primate one (Sone et al., 2003). Eventually, by contrast to the highly efficient production (>90%) of vascular endothelial cells from murine ES cells (Hirashima et al., 1999), that from primate ES cells is significantly low; the efficiency of the production of vascular endothelial cadherin (VE-cadherin)-positive (Sone et al., 2003, 2007) or platelet endothelial cell adhesion molecule-1 (PECAM-1)-positive (Levenberg et al., 2002) cell are not higher than two percents. Although the human ES cell study is essential for clinical application, basic researches using monkey ES cells still has great importance because they provide good transplantation models that must be performed in the pre-clinical study (Takagi et al., 2005). Moreover, the use of monkey ES cells avoids ethical issues and thus the biotechnological manipulation of them, including gene transfer, can immediately be applied, which will contribute to understand human ES cells.

Currently, there are three major methods for the in vitro differentiation of ES cells into specific lineages. One is co-culturing ES cells with stromal cells as their feeders (Hirashima et al., 1999; Sone et al., 2003, 2007). Feeder cells have large capacities to promote directed differentiation and to support viability of differentiated cells. Nevertheless, contamination of the final product by feeder cells is inevitable, and thus, an especially strict cell-sorting technique is required for purification of the final products. Concerning vascular endothelial differentiation of primate ES cells, however, the efficiency of cell surface VE-cadherin-positive cell production is considerably low (<2%) even when murine OP9 feeder cells were used (Sone et al., 2003, 2007). Besides, massive

Contract grant sponsor: The Japan Health Sciences Foundation; Contract grant number: KH61061.

*Correspondence to: Akira Yuo, Department of Hematology, Research Institute, International Medical Center of Japan, 1-21-1, Toyama, Shinjuku-ku, Tokyo 162-8655, Japan.
E-mail: yuoakira@ri.imcj.go.jp

Received 22 December 2007; Accepted 23 April 2008

DOI: 10.1002/jcp.21502

contamination of pericytes reportedly occurs in this system. Pericytes are important players for angiogenesis, and thus, the co-generation of pericytes might be beneficial in some aspects. However, domination of pericytes after passages considerably hinder the pure expansion of vascular endothelial cells even after sorting of VE-cadherin-positive cells (Sone et al., 2007). The second method is a feeder-free culture via a generation of embryoid bodies (EBs) or spheres (Levenberg et al., 2002). It is beneficial that it can exclude the risk of contamination of xenogenic materials. Yet, directions of differentiation in EBs or spheres are principally random and cannot easily be focused on a specific lineage. As a result, fairly large volumes of starting ES cells are required to obtain sufficient amounts of differentiated cells. Additionally, these two methods described above share a common disadvantage; they do not provide a clear microscopic field for observation and manipulation due to co-existing feeder cells or the compact three-dimensional structures of EBs or spheres. The third method is a simple adherent culture of ES cells. There have been two reports concerning this method. One is the continual culture of rhesus monkey ES (rmES) cells on mouse embryonic fibroblasts (MEFs) using a vascular endothelial cell-specific culture medium of EGM®-2 MV BulletKit (Kaufman et al., 2004). This system provided a good microscopic field and effectively produced the subculturable vascular endothelial cells. However, these cells are not the conventional or canonical vascular endothelial cells, but rather, seem to be "atypical" vascular endothelial cells in that neither the expression of VE-cadherin, a vascular endothelial cell-specific and pan-vascular endothelial marker, nor PECAM-1, a mature vascular endothelial cell marker, was detected by flow cytometry. Nonetheless, they have mature endothelial functions including in vitro cord-forming and acetylated low density lipoprotein (Ac-LDL)-uptaking activities and in vivo neovascularization activity along with expressions of von Willbrand factor (vWF) and endothelial nitric oxide synthetase (eNOS). The other one is an adherent culture of human ES-derived CD34-positive cells, which were spontaneously generated by overgrown ES cells on MEFs in the presence of serum, in EGM®-2 MV BulletKit (Wang et al., 2007). This system requires the enrichment of CD34-positive cells (<10%) by cell sorter before subsequent culture in EGM®-2 MV BulletKit. Although this system provides VE-cadherin-positive functional vascular endothelial cells, they are not subculturable. Thus, the most urgent task for the vascular endothelial differentiation from primate ES cells is to establish a method for "feeder-free" and "high efficiency" production for cell surface "VE-cadherin-positive" and "subculturable" vascular endothelial cells.

Here we report a novel method for highly efficient production of functional, subculturable, freeze–thaw-tolerable and cell-surface-VE-cadherin-positive vascular endothelial cells from cynomolgus monkey ES (cmES) cells in feeder-free culture system. Furthermore, it does not require a step to enrich the progenitor fractions, such as CD34-positive and/or KDR-positive fractions, by cell sorter. To our knowledge, this is the highest efficiency system for the production of vascular endothelial cells. Indeed, our system provides almost two pure populations: the cell surface VE-cadherin-positive canonical vascular endothelial cells and cell surface VE-cadherin-negative "atypical" vascular endothelial cells. The characterization and significance of these atypical vascular endothelial cells is referred and discussed in this report.

Materials and Methods

Cells and reagents

Murine embryonic fibroblasts (MEFs), which had been treated with Dulbecco's modified Eagle's medium (DMEM) containing mitomycin C (MMC) (Sigma Chemical Co., St. Louis, MO) for 3 h, were seeded on the dishes coated with 0.1% gelatin. The cmES cells (CMK-6) (Suemori et al., 2001) were maintained on MMC-treated MEF-coated dishes in DMEM/F12 medium (Invitrogen Corp., Carslbad, CA) supplemented with 20% Knockout™ Serum Replacement (KSR™, Invitrogen Corp.), 1% Non-essential amino acids solution (Invitrogen Corp.), 1 mM Sodium Pyruvate Solution (Invitrogen Corp.), 2 mM L-glutamine (Invitrogen Corp.), 10 U/ml penicillin (Invitrogen Corp.) and 10 μg/ml streptomycin (Invitrogen Corp.). ES cells were passed twice a week by collagenase treatment and seeded at split ratios of 1:2 to 1:4 on new MEF-coated dishes. Human aortic endothelial cells (HAEC) and human umbilical vein endothelial cells (HUVEC) were purchased from Lonza Group Ltd. (Basel, Switzerland), and maintained on gelatin-coated dishes using EGM®-2 BulletKit (Lonza Group Ltd.). Normal Human Aortic Smooth Muscle cells (AOSMC)) were purchased from Lonza Group Ltd. and maintained on gelatin-coated dishes using SmGM®-2 BulletKit® (Lonza Group Ltd.). The human leukemic UT-7 and HL-60 cells were cultured RPMI 1640 medium (Sigma Chemical Co.) supplemented with 10% heat-inactivated fetal bovine serum (FBS).

Differentiation procedure

ES colonies were collected by collagenase treatment without a contamination of MEFs and further disaggregated by trypsinization. Cell aggregates were generated by a hanging drop culture, where 3,000 cmES cells were incubated in a 30 μl drop of differentiation medium (DM) consisting of Iscove's modified Dulbecco's medium (IMDM) (Sigma Chemical Co.) supplemented with 15% heat-inactivated FBS (PAA Laboratories GmbH, Linz, Austria), 0.1 mM β-mercaptoethanol (Sigma Chemical Co.), 3 mM L-glutamine (Invitrogen Corp.), 10 U/ml penicillin (Invitrogen Corp.), 20 ng/ml vascular endothelial growth factor (VEGF; Pepro Tech Inc., Rocky Hill, NJ), 20 ng/ml bone morphogenic protein 4 (BMP-4; R&D Systems Inc., Minneapolis, MN), 20 ng/ml stem cell factor (SCF; Pepro Tech Inc.), 10 ng/ml Flt3 ligand (Flt3-L; Pepro Tech Inc.), 20 ng/ml interleukin 3 (IL-3; Pepro Tech Inc.) and 10 ng/ml interleukin 6 (IL-6; Pepro Tech Inc.). After incubating the drops for 3 days at 37°C under a 100% humidified condition in a 5% CO_2 gas incubator, cell aggregates generated from 72 hanging drops were subjected to adherent culture on a 100 mm × 20 mm gelatin-coated dishes using differentiation medium described. Media were changed twice a week. After about 2 weeks, a VE-cadherin-positive sac-like structure filled with round cells along with surrounding VE-cadherin-positive cobblestone cells emerged. Before sacs were fully packed by inner round cells, sac walls were manually cut by using stem cell knife (Vitrolife AB, Kungsbacka, Sweden) under microscopic observation. After releasing the inner round cells into culture supernatant, total adherent cells including fragmented sac walls and surrounding cobblestone cells were massively transferred onto new gelatin-coated dishes via trypsin/EDTA treatment. These cells were subcultured by 1:3 dilution twice a week. In some experiments, EGM®-2 BulletKit (Lonza Group Ltd.) was used in place of the differentiation medium described above throughout the differential processes including hanging drop culture and subsequent adherent culture.

Morphological and cytochemical examinations

Viable cells were directly observed under an inverted phase contrast light microscope (Olympus Optical Co. Ltd., Tokyo, Japan), or alternatively, cells were fixed on slide glasses using a cytospin apparatus (Cytospin 2, SHANDON, Pittsburgh, PA), stained with Wright-Giemsa solution, myeloperoxidase staining kit or esterase staining kit (Muto Pure Chemical Co., Tokyo, Japan), and then observed under the light microscope (Olympus Optical Co. Ltd.).

Flow cytometric analyses and cell sorting

Cells were collected by 0.2% EDTA treatment and, after a wash in phosphate-buffered saline (PBS), 1×10^6 cells were reacted with first antibodies on ice for 30 min. The expression level of each protein was analyzed using a FACSCalibur™ (BD Biosciences, San Jose, CA). The antibodies used were a mouse monoclonal anti-human VE-cadherin (clone TEA1/31)-phycoerythrin (PE) antibody (Beckman Coulter Inc., Fullerton, CA), a mouse monoclonal anti-human CD31 (PECAM-1)-fluorescein isothiocyanate (FITC) antibody (clone WM59) (BD Biosciences), a mouse monoclonal anti-human CD34 (clone 563)-PE antibody (BD Biosciences), a mouse monoclonal anti-human Tie-2 (clone 83715)-PE (R&D Systems Inc.), a mouse monoclonal anti-human VEGF-R1 (Flt-1) (clone 49560)-PE antibody (R&D Systems Inc.), a mouse monoclonal anti-human VEGF-R2 (KDR, Flk-1) (clone 89106)-PE antibody (R&D Systems Inc.), a mouse monoclonal anti-human VEGF-R3 (Flt-4) (clone 54733)-PE antibody (R&D Systems Inc.), a mouse monoclonal anti-human CD14 (clone M5E2)-PE antibody (BioLegend, San Diego, CA), a mouse monoclonal anti-human CD18 (clone 6.7)-FITC antibody (BD Biosciences), a mouse monoclonal anti-human CD11b (clone ICRF44)-PE antibody (BD Biosciences) and a mouse monoclonal anti-human CD45 (clone TÜ116)-PE antibody (BD Biosciences). As for the anti-VE-cadherin antibody reaction, secondary antibody reaction was performed using a goat anti-mouse IgG-PE (Calbiochem Co., La Jolla, CA). After antibody-staining procedures, cells were stained with TO-PRO3 fluorescent dye (Invitrogen Corp.) for 10 min. During analysis, dead cells were gated out as the FL4-higher fraction. The cell surface VE-cadherin-positive and VE-cadherin-negative fractions were sorted using as FACSAria™ (BD Biosciences) after cells were stained VE-cadherin (clone TEA1/31)-phycoerythrin (PE) antibody (Beckman Coulter Inc.).

Immunostaining

The cells were fixed on slide glasses with a cytospin apparatus (Cytospin 2) with further fixation with acetone/methanol solution (1:3). The immunostaining procedure was performed as described elsewhere (Saeki et al., 2003) with first antibody reactions using a mouse anti-human VE-cadherin antibody (clone55-7H1) (BD Biosciences), a rabbit anti-human N-cadherin antibody (H-63) (Santa Cruz Biotechnology Inc., Santa Cruz, CA), a rabbit polyclonal anti-human Nanog antibody (ReproCELL Inc., Tokyo, Japan), a mouse monoclonal anti-human Actin, α smooth muscle (SMA) (clone 1A4) (Sigma Chemical Co.), a mouse monoclonal anti-platelet-derived growth factor receptor β (PDGF-Rβ (clone 28) (BD Biosciences), a rabbit polyclonal anti-human eNOS antibody (H-159) (Santa Cruz Biotechnology Inc.), a goat polyclonal anti-human vWF antibody (C-20) (Santa Cruz Biotechnology Inc.) or a mouse monoclonal anti-CD68 antibody (Transgenic Inc., Kobe, Japan) followed by second antibody reactions using Alexa Fluor® 488 chicken anti-mouse IgG (H + L), Alexa Fluor® 568 goat anti-rabbit IgG (H + L) or Alexa Fluor® 594 chicken anti-goat IgG (H + L) (Molecular Probes, Inc., Eugene, OR).

Cord formation assays

Matrigel (BD Biosciences) was loaded into the 24 multi-well dishes (95 μl/well). After the dishes were incubated for 30 min at 37°C, 1×10^4 cells per well were seeded in 1 ml of EGM®-2 BulletKit supplemented with cytokines and growth factors according to the manufacturer's instructions (Cambrex Bio Science Walkersville, Inc., Walkersville, MD). Cell morphologies were observed after overnight culture under an inverted light microscope (Olympus Optical Co. Ltd.).

Colony assays

Colony assays were performed using Methocult TM GF^+H4535 (Stemcell Technologies Inc., Vancouver, Canada) according to the manufacturer's recommendations. In brief, 0.3 ml of cell suspension, which contained 10 cells, was mixed in 3 ml of methylcellulose solution consisting of 1% methylcellulose, 30% FBS, 1% bovine serum albumin, 0.1 mM β-mercaptoethanol, 2 mM L-glutamine, 50 ng/ml SCF (Pepro Tech Inc.), 20 ng/ml IL-3 (Pepro Tech Inc.), 20 ng/ml IL-6 (Pepro Tech Inc.), 20 ng/ml granulocyte-macrophage colony-stimulating factor (GM-CSF; Pepro Tech Inc.), 20 ng/ml granulocyte colony-stimulating factor (G-CSF; Kirin Brewery Company, Ltd., Tokyo, Japan) and 3 U/ml erythropoietin (Kirin Brewery Company, Ltd.) in 3.5-cm culture dishes. After 2 weeks, the number of colonies was counted. The morphology of the colonies was observed under an inverted light microscope (Olympus Optical Co. Ltd.).

Western blotting

Western blotting was performed as described previously (Saeki et al., 2003) using a rabbit anti-human VE-cadherin antibody (C-19) (Santa Cruz Biotechnology Inc.) or a mouse monoclonal anti-tubulin β (D-10) antibody (Santa Cruz Biotechnology Inc.). The second antibody reaction was performed using a horseradish peroxidase-conjugated anti-rabbit or anti-mouse IgG (Cell Signaling Technology, Inc., Beverly, MA). The final detection procedure was performed using ECL Western blotting detection reagents (GE Healthcare UK Ltd., Buckinghamshire, England).

Uptake of acetylated low-density lipoprotein (Ac-LDL)

Cells were transferred in 4-well chamber slide system (Nalge Nunc International Corp., Naperville, IL). After overnight culture, cells were washed by Hank's balanced salt solution (HBSS) twice and incubated in serum-free medium containing 10 μg/ml of low-density lipoprotein from human plasma, acetylated, DiI complex (DiI Ac-LDL) (Molecular Probes) for 4 h. After washing the cells by HBSS for three times, the cells were observed under the fluorescence microscope (Olympus Optical Co. Ltd.).

Polymerase chain reaction (PCR)

Genomic PCR. Genomic DNA was extracted from ES-derived vascular endothelial cells (ESdEC), HUVECs (Cambrex Bio Science Walkersville, Inc.) or MEFs of the ICR stain (CLEA Japan, Inc., Tokyo, Japan). 1×10^6 cells were lysed with a buffer (50 mM Tris–HCl (pH 8.0), 0.1 M NaCl, 20 mM EDTA and 0.1% SDS) supplemented with 75 μg/ml Proteinase K (WAKO Pure Chemical Industries, Osaka, Japan) for 8 h at 55°C. After phenol/chloroform extraction and isopropanol precipitation, dried pellets were solubilized by 100 μl of water containing 50 ng/ml DNase-free RNase (Invitrogen Corp.) and incubated for 1 h at 37°C. The genomic DNA solution was kept at −80°C. PCR was performed using 2 μl of the 50× diluted DNA template, SP-Taq (Hokkaido System Science Co., Ltd., Hokkaido Japan) and following primers. For detecting the murine ly 9.2 genomic fragment, a forward primer 5′-gtaaattcccccagccttgt-3′ and a reverse primer 5′-atgccatgtcctcttcatccs-3′ were used (the product length is 433 bp). For detecting the primate CD34 genomic fragment, a forward primer 5′-CGACAGTCAAATTCACATCTACC-3′ and a reverse primer 5′-GAGATGTTGCAAGGCTAGTGC -3′ were used (the product length is 254 bp). The PCR procedure was carried out using a DNA Thermal Cycler PJ2000 (PerkinElmer Corp., Foster City, CA) with the following program: 95°C; 5 min, 94°C; 30 sec, 57°C; 30 sec, 72°C; 1 min at 27 cycles for murine ly9.2 and at 34 cycles for primate CD34. The product was separated by agarose gel electrophoresis and the DNA was visualized by ethidium bromide staining. A 100 bp ladder marker 4 (Nippon Gene Co. Ltd., Tokyo, Japan) was used to evaluate the molecular weights of the PCR products.

Reverse transcription-polymerase chain reaction (RT-PCR). RNA was extracted from 5×10^6 cells with RNeasy Mini Kit (Qiagen Inc., Valencia, CA) and cDNA was synthesized by Superscript II Kit (Invitrogen Corp.) according to a manufacture's protocol. The PCR procedure was carried out as described above using primate globin-ε primers; a forward primer 5′-TGCATTTTACTGCTGAGGAGA-3′ and a reverse primer 5′- AAGAGAACTCAGTGGTACTT-3′, primate globin-ζ primers; a forward primer 5′-TTCCTCAGCCACCCGCAGAC-3′ and a reverse

primer 5′-AGCAGGCAGTGGGACAGGAG-3′, primate VE-cadherin primers; a forward primer 5′-TGGGCTCAGACATCCACATA-3′ and a reverse primer 5′-TCACAGTCTCCCTTGGGAAT-3′. For internal control, primate β-actin primers were used: a forward primer 5′-gCAggAgATggCCACggCgCC-3′ and a reverse primer 5′-TCTCCTTCTgCATCCTgTCggC-3′.

Collagen plug assay

About 10 blocks of dried honeycomb collagen sponge (Koken Co. Ltd., Tokyo, Japan) were mixed with 500 μl of cmES-derived cells at passage number 4, which were suspended in differentiation medium at the density of 4×10^5/ml, and were then cultured for 2 days in vitro. Then they were transplanted intraperitoneally into SCID mice. After 35 days, 0.2 ml of FITC-dextran (500,000 average molecular size, Sigma Chemical Co.) solution (100 mg FITC-dextran suspended in 5 ml PBS) was injected into mice from a tail vein. After several minutes, mice were sacrificed and the blocks were fixed by 10% formaldehyde and paraffin embedded. The 4 μm sliced specimen were further subjected to immunostaining using a mouse monoclonal anti-human HLA-A, B, C antibody (BD Biosciences) or a rabbit polyclonal anti-PECAM-1 antibody (H-300) (Santa Cruz Biotechnology Inc.), and also to histological examination using hematoxylin and eosin solutions.

Results

A sac-like structure with surrounding cobblestone cells as a parental organization for vascular endothelial cell generation

During our attempt to generate hematopoietic progenitor cells from cmES cells under feeder-free conditions, we found that the condition we had tried to optimize for hematopoietic differentiation was unexpectedly fitted for the production of vascular endothelial cells. Our differentiation medium was prepared by modifying the one reported in a case of hematopoietic differentiation of rmES cells by co-culture method (Li et al., 2001). In the presence of VEGF, BMP-4, SCF, Flt3-L, IL-3, IL-6 and serum, we generated spheres from cmES cells (Fig. 1A,B, upper left). Then spheres were subjected to adherent culture on gelatin-coated dishes (Fig. 1A,B, upper middle and right). Time course observations revealed the differentiation processes as follows: spreading of cobblestone-shaped cells with leaving the center region rather amorphous in a few days (Fig. 1B, lower left); swelling of the center region at about 6 days (Fig. 1B, lower middle); ballooning out of the center region resulting in the formation of "a sac-like structure" filled with abundant round cells, some of which brimmed over the sac wall, around 12 days (Fig. 1B, lower right). At this time, the cobblestone cells were divided into two populations by their morphology. The cells located at proximal regions to the sac-like structure became densely packed, while the cells located at distal regions remained rather stretched (Fig. 1C). Although the early phased cobblestone cells (Fig. 1B, lower left) did not express VE-cadherin but expressed only N-cadherin at intercellular junctions (data not shown), VE-cadherin expression had become detectable in all adherent cells at the time when a sac-like structure was formed. As shown in Figure 1D, the late phased cobblestone cells, including proximal compact cells and distal extended cells, as well as sac wall cells expressed VE-cadherin at intercellular junctions. Thus, total adherent cells generated after the culture of ES-derived spheres on gelatin-coated dishes using our differentiation medium are regarded as vascular endothelial cell-committed populations although no special selection procedures were performed.

We also studied the characteristics of the non-adherent round cells, majority of which located within the sacs and minor portion of which resided around the sacs. They were collected from the culture supernatant after cutting the sac walls by micropipettes and releasing into the medium. The cytochemical analysis including Wright-Giemsa, myeloperoxidase and esterase staining showed that the majority of the round cells were myeloblasts and macrophages (Fig. 1E). This finding was further supported by the results of colony assays of round cells, where generation of granulocyte/macrophage colonies consisting of promyelocytes, myelocytes, and segmented neutrophils were observed (Fig. 1F). Because sac-like structures resembled the morphology of blood islands in the yolk sac, we investigated the possible existence of primitive hematopoietic cells. The RT-PCR studies showed that the messages for embryonic hemoglobins, globin-ε and globin-ξ, were expressed at the sac stage (Fig. 1G, lane 2 (cmES-derived cells, p1)) and subsequent first-passage-stage (Fig. 1G, lane 3 (cmES-derived cells, p2)). Thus, non-adherent round cells consist of myeloblasts and macrophages along with a small portion of primitive erythroid cells.

Hence, simple adherent culture of ES-derived spheres in the presence of hematopoietic cytokines resulted in generation of a unique construction: a sac-like structure and surrounding cobblestone cells that expressed VE-cadherin along with primitive and definitive hematopoietic cells localized within and around the sac.

Characterization of subcultured adherent cells

We next tried to expand the cell surface VE-cadherin-positive adherent cells by an ordinary subculture method. After cutting sac walls and releasing the inner hematopoietic cells into culture supernatant, residual adherent cell populations including sac wall-constituting cells and surrounding cobblestone cells were detached by trypsin/EDTA treatment and transferred massively onto new gelatin-coated dishes. During the cutting process of the sac walls, they were divided into small fragments but remained attached to dishes. After trypsin/EDTA treatment, the cells were dissociated almost into single cell and transferred to new gelatin-coated plates by 1:3 dilution. Cells actively proliferated and reached confluence in 3–4 days. They showed highly homogenous spindle-shaped morphology similar to HUVEC (Fig. 2A). Indeed, these cmES-derived cells showed cord-forming activities equivalent to HUVEC (Fig. 2B). Furthermore, all of the cells were positive for Ac-LDL-uptaking activities (Fig. 2C) with uniform expressions of eNOS and vWF (described in the following part of the manuscript and Fig. 4B, left parts).

To quantitatively evaluate the vascular endothelial differentiation, we determined the cell surface expression of VE-cadherin and PECAM-1 by flow cytometry. As shown in Figure 3A, limited populations were positive for VE-cadherin and PECAM-1 despite rather uniform expression of VE-cadherin before subculture (Fig. 1D). Although the reason for the reduction of VE-cadherin expression after subculture was not known, the expressions of VE-cadherin/PECAM-1 were well preserved during subsequent culture (Fig. 3B). The cells were subculturable up to eight passages, during which 2×10^5 cmES cells generated 7×10^9 of VE-cadherin/PECAM-1-positive vascular endothelial cells. Moreover, the cells were freeze–thaw-tolerable and re-cultured cells properly retained the VE-cadherin/PECAM-1 expressions (Fig. 3C). The average percents of VE-cadherin/PECAM-1-positive cells were $29.8 \pm 15.1\%$ ($n = 17$). The expressions of other surface markers for vascular endothelial cells were also examined. As shown in Figure 3D, the expression of VEGF-R1, a vascular endothelial cell-specific marker, was detected at a comparable level to HUVEC and HAEC. Tie-2 expression was also detected in cmES-derived cells although the expression levels were slightly lower than HUVEC and HAEC. On the other hand, CD34-positive populations were detected mainly in cmES-derived cells and HUVEC. Interestingly, the expression of

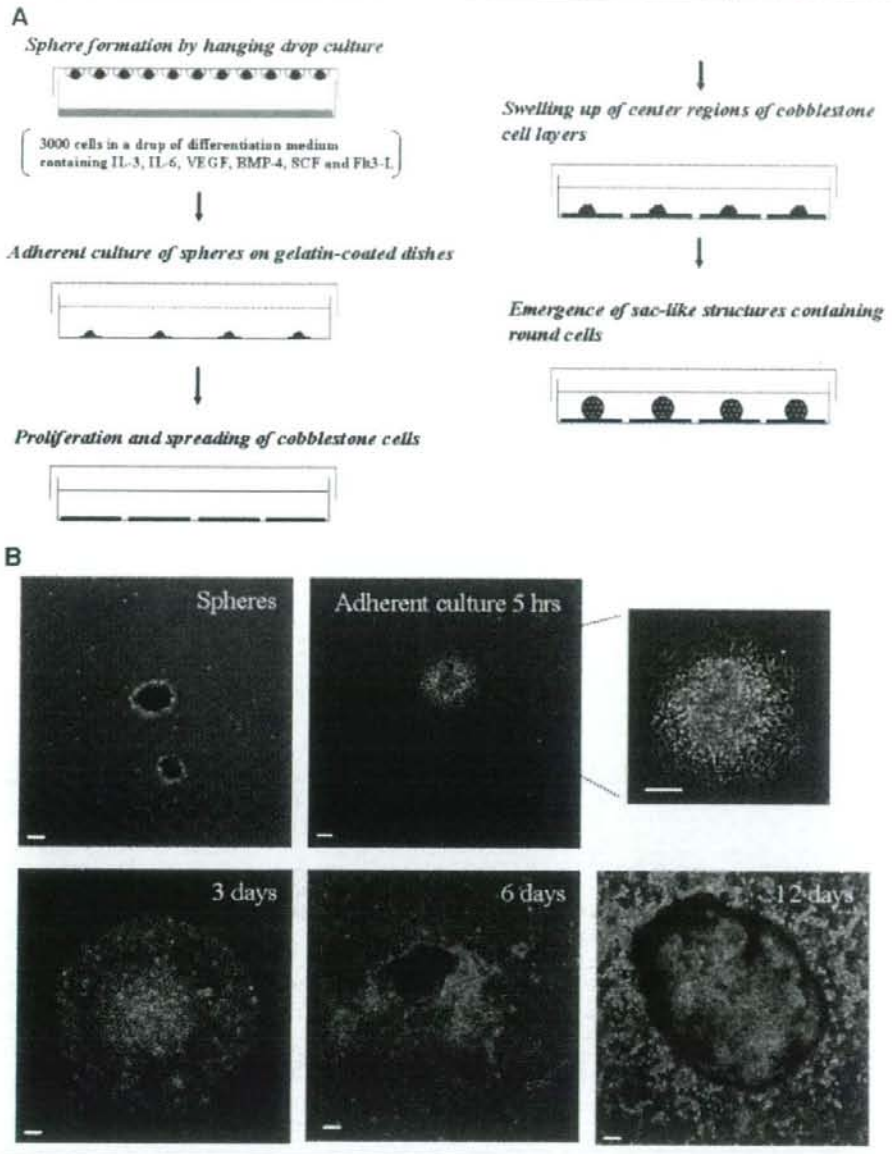

Fig. 1. Generation of a sac-like structure and cobblestone cells from feeder-free differentiation culture of cmES cells. The procedure for the production of a sac-like structure (A) and phase contrast microscopy (B). Spheres were generated by a hanging drop culture and subjected to subsequent adherent culture using gelatin-coated plates. Within a few days, spheres adhered on the plates became flattened and VE-cadherin-negative cobblestone cells spread out. At about 6 days, the center region began to swell up again. Around 12 days, the center regions ballooned out and sac-like structures were formed. Scale bars indicate 100 μm. C: The phase contrast microscopy of late phase cobblestone cells. Morphologies of proximal and distal cobblestone cells that surrounded a sac-like structure were shown. The scale bar indicates 100 μm. D: VE-cadherin expression in late phase cobblestone cells. Sac-like structure and surrounding cobblestone cells were stained with anti-VE-cadherin antibody. The scale bar indicates 50 μm. E: Morphological and cytochemical examinations of the round cells released from the sac-like structure. The Wright-Giemsa staining (WG) showed the presence of two types of the cells: the small cells with basophilic cytoplasm and high nucleus/cytoplasm ratio resembling myeloblasts and the large cells with abundant vacuolated cytoplasms resembling macrophages. The myeloperoxidase staining (MPO) showed that majority of the small cells were positive for myeloperoxidase. The esterase double staining (Esterase) showed the cells with blue granules (granulocyte lineage cells) and cells with brown granules (macrophage lineage cells). The scale bar indicates 100 μm. F: Hematopoietic colony assays. The round cells released from the sac-like structure were subjected to hematopoietic colony assays. The phase contrast microscopic observation (Phase) showed the presence of granulocyte/macrophage colonies. Wright-Giemsa staining (WG) of the cells from colonies showed the presence of myeloblasts (a black arrow), promyelocytes (a blue arrow) and polymorphonuclear granulocytes (a red arrow). The myeloperoxidase staining (MPO) showed the presence of a myeloperoxidase-rich smaller granulocyte population (a black arrow) and a myeloperoxidase-poor large macrophage population (a red arrow). Esterase double staining (Esterase) showed the presence of cells with blue granules (a black arrow) and cells with brown granules (a red arrow). The scale bar indicates 100 μm. G: RT-PCR. The presence of primitive hematopoietic cells was shown by the existence of messages for embryonic hemoglobins (globin-ε and globin-ζ) using primate-specific primers (pr-globin-ε, pr-globin-ζ, and pr-β-actin). "M" indicates 100 bp ladder marker. The subscript character of "p" of cmES-derived cells indicates the passage number. "H"; HUEVC, "E"; undifferentiated cmES cells, "U"; hematopoietic UT-7 cells as positive control. [Color figure can be viewed in the online issue, which is available at www.interscience.wiley.com.]

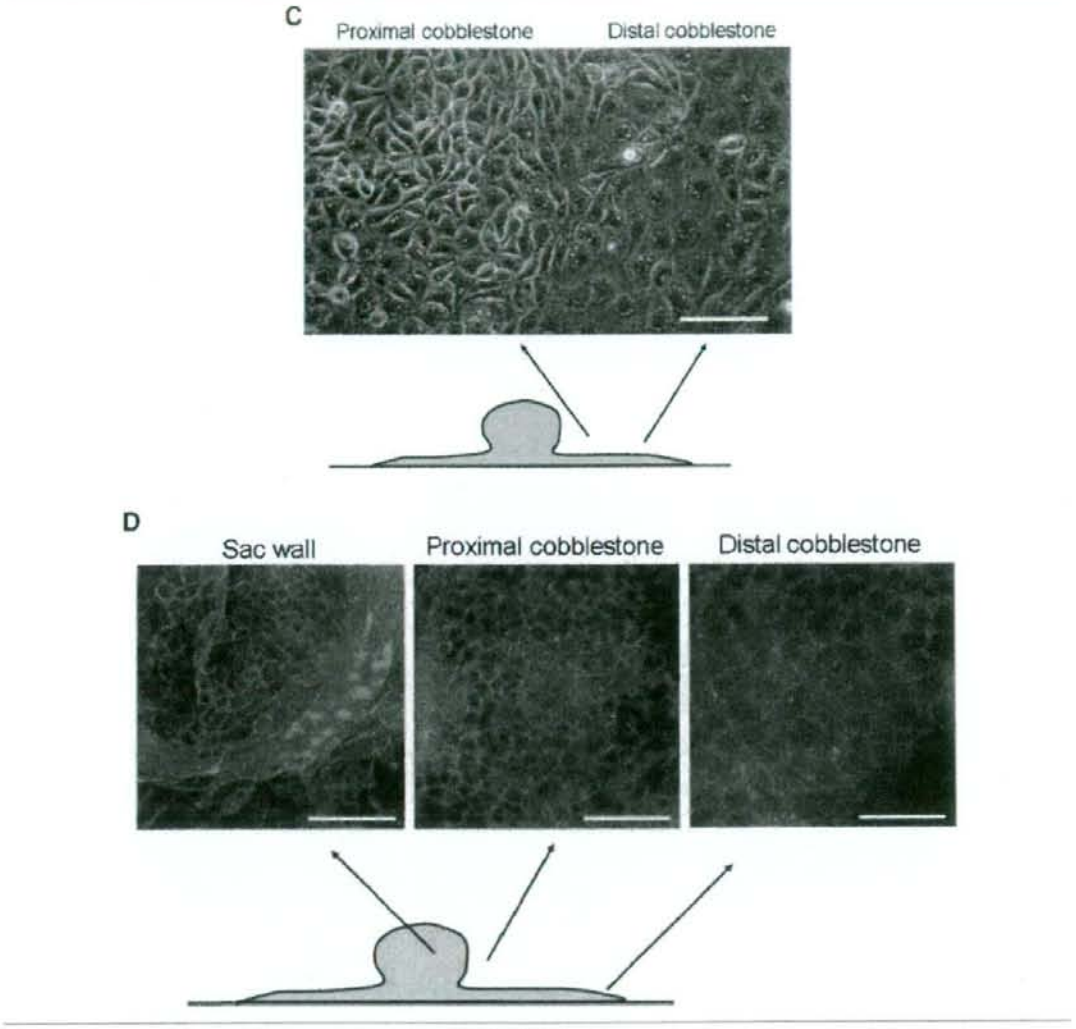

Fig. 1. ***(Continued)***

VEGF-R3, a marker for lymphatic endothelial and embryonic vascular endothelial cells, was detected at fairly high levels in cmES-derived cells and HUVEC. The expression of VEGF-R2, a marker for vascular and lymphatic endothelial cells, was constantly detected at the same level as VE-cadherin, as we confirm it by detailed analyses in the following part of the manuscript (Fig. 5). From these flow cytometric analyses, it was concluded that cmES-derived cells resembled HUVEC rather than HAEC.

Although limited populations of cmES-derived cells were positive for cell surface VE-cadherin/PECAM-1, their uniform Ac-LDL-uptaking activities and uniform expressions of eNOS and vWF, taken together with their cord-forming activities and VEGF-R1 expression equivalent to HUVEC, suggest that the almost all of the cmES-derived cells are vascular endothelial cells or vascular endothelial endothelial-like cells and, therefore, "VE-cadherin/PECAM-1-negative" populations are also types of cells that are closely related to the vascular endothelial cells. This idea was analogous to the proposal by Thomson and colleagues (Kaufman et al., 2004). They showed that rmES-derived vascular endothelial cells were negative for VE-cadherin/PECAM-1 despite the presence of mature endothelial functions with eNOS and vWF expressions. They used commercially available EGM®-2 BulletKit for the differentiation of rmES cells. Eventually, usage of EGM®-2 BulletKit resulted in the production of almost pure VE-cadherin/PECAM-1-negative vascular endothelial cells by our method as the report by Thomson and colleagues. As shown in Figure 4, differentiation induction by our method using EGM®-2 BulletKit resulted in generation of cells with mature

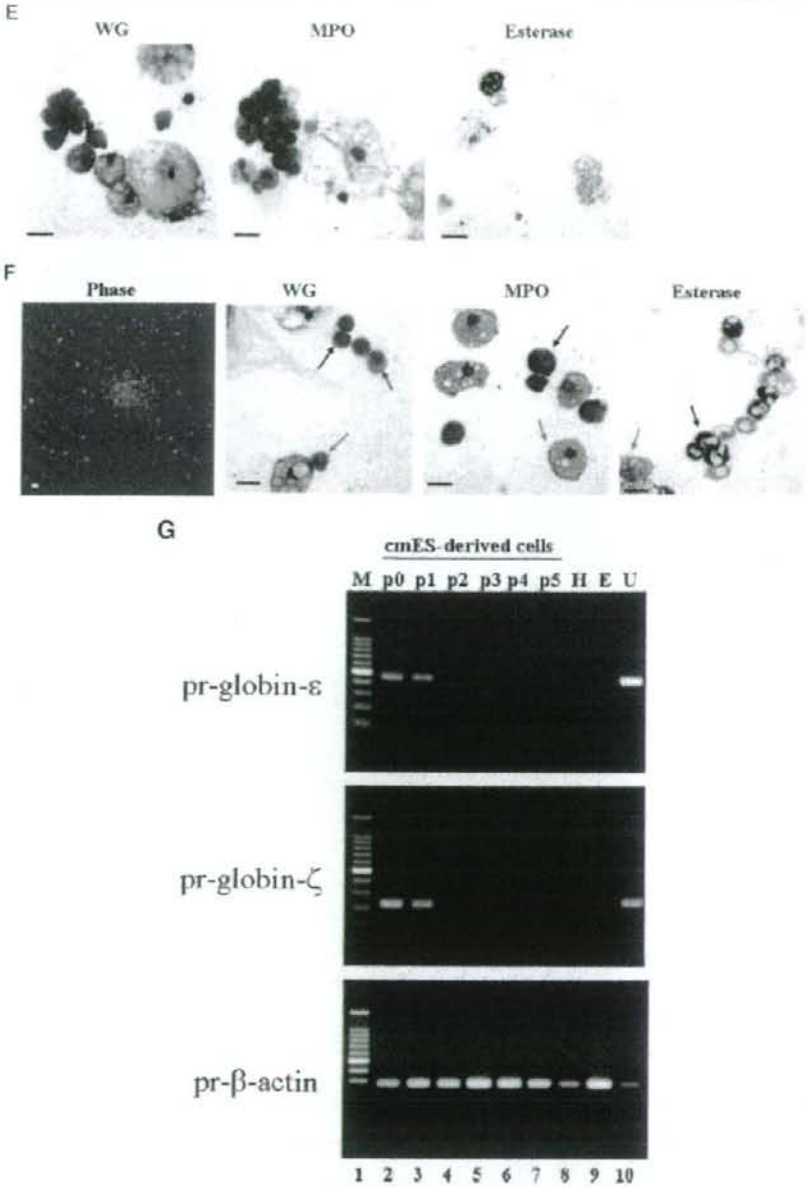

Fig. 1. (*Continued*)

functions including cord-forming activities (Fig. 4A, upper right in EGM2 part) and uniform Ac-LDL-uptaking activities (Fig. 4A, middle and lower right in EGM2 part) and with eNOS and vWF expressions (Fig. 4B, EGM2 part) despite the lack of VE-cadherin/PECAM-1 as assessed by flow cytometry (Fig. 4A, lower left in EGM2 part). In contrast to the findings by Thomson and colleagues (Kaufman et al., 2004), VE-cadherin expression was detected by Western blotting (Fig. 4C) in our culture system even by using EGM®-2 BulletKit, indicating that VE-cadherin protein was really produced though its membrane translocation seems to be blocked by unknown reason(s). Anyway, it can be concluded that there existed an "atypical"

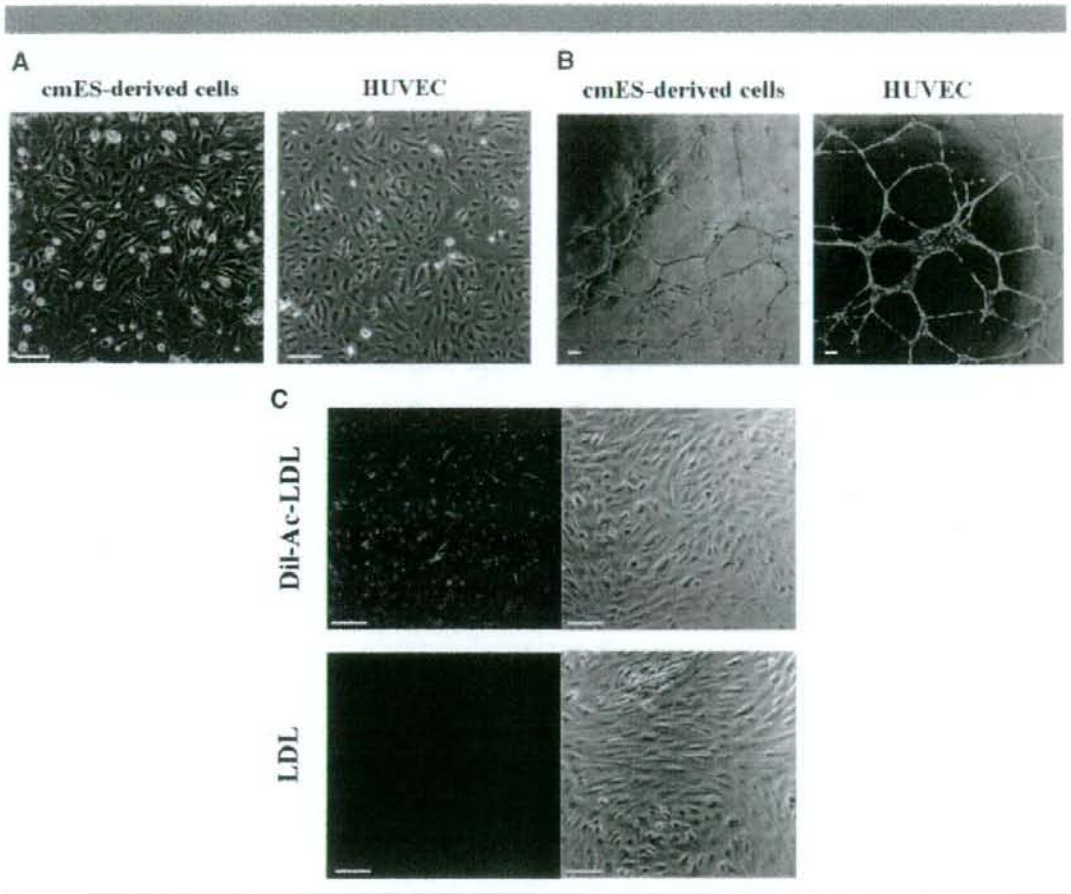

Fig. 2. Morphology and functions of cmES-derived subcultured cells. A: The phase contrast microscopy. Morphologies of cmES-derived cells (left) and HUVEC (right) were shown. The scale bar indicates 100 μm. B: Cord formation assays. A cord-forming activity of cmES-derived cells (left) and HUVEC (right) was shown. The scale bar indicates 100 μm. C: Ac-LDL-uptaking assays. Fluorescence (DiI)-labeled Ac-LDL (upper) or non-labeled LDL (lower) was added to cmES-derived cells. After overnight culture, cells were observed under fluorescence microscopy. Right parts indicate the photographs with Normarsky differentiated interference contrast. The scale bar indicates 20 μm.

type of vascular endothelial cells (i.e., cell surface VE-cadherin/PECAM-1-negative vascular endothelial cells) among primate ES-derived differentiated cells.

For further understanding of cell surface VE-cadherin-positive "canonical" vascular endothelial cells and cell surface VE-cadherin-negative "atypical" vascular endothelial cells, we fractionated those two populations by FACSAria. As shown in Figure 5C, cell surface VE-cadherin-positive populations proliferated as VE-cadherin-positive cells and expanded by 160-fold after five passages. Interestingly, cell surface VE-cadherin-positive populations were positive for cell surface CD34 expression as assessed by flow cytometry (Fig. 5D). The immunostaining study of cell surface VE-cadherin-positive cells clearly showed the localization of VE-cadherin at intercellular junctions in these cells (Fig. 5E). The functional maturation including cord-forming activities (Fig. 5F) and uniform Ac-LDL-uptaking activities (Fig. 5G) was also detected in cell surface VE-cadherin-positive populations. Expressions of other vascular endothelial markers were also detected including VEGF-R1, VEGF-R2, VEGF-R3, and Tie-2 (Fig. 5H). On the other hand, the cell surface VE-cadherin-negative populations proliferated as VE-cadherin-negative cells and were negative for cell surface CD34 expression (Fig. 6A–D). Interestingly, these cells showed obvious cord-forming capacities (Fig. 6E) and a uniform Ac-LDL-uptaking activity (Fig. 6F). Moreover, they expressed VEGF-R1, VEGF-R3, and Tie-2 despite the absence of VEGF-R2 as demonstrated by flow cytometric analyses (Fig. 6G). Immunostaining studies using an anti-VE-cadherin antibody demonstrated intracellular region-staining patterns (Fig. 6H), suggesting that the cell surface VE-cadherin-negative cells expressed VE-cadherin intracellularly. This finding was confirmed by Western blotting studies, which showed the presence of the 130-kDa VE-cadherin band (Fig. 6I). RT-PCR studies further demonstrated the presence of the VE-cadherin message (Fig. 6J). As monocytes/macrophages or other hematopoietic cells reportedly show various endothelial cell-like features and are positive for VEGF-R1 and VEGF-R3

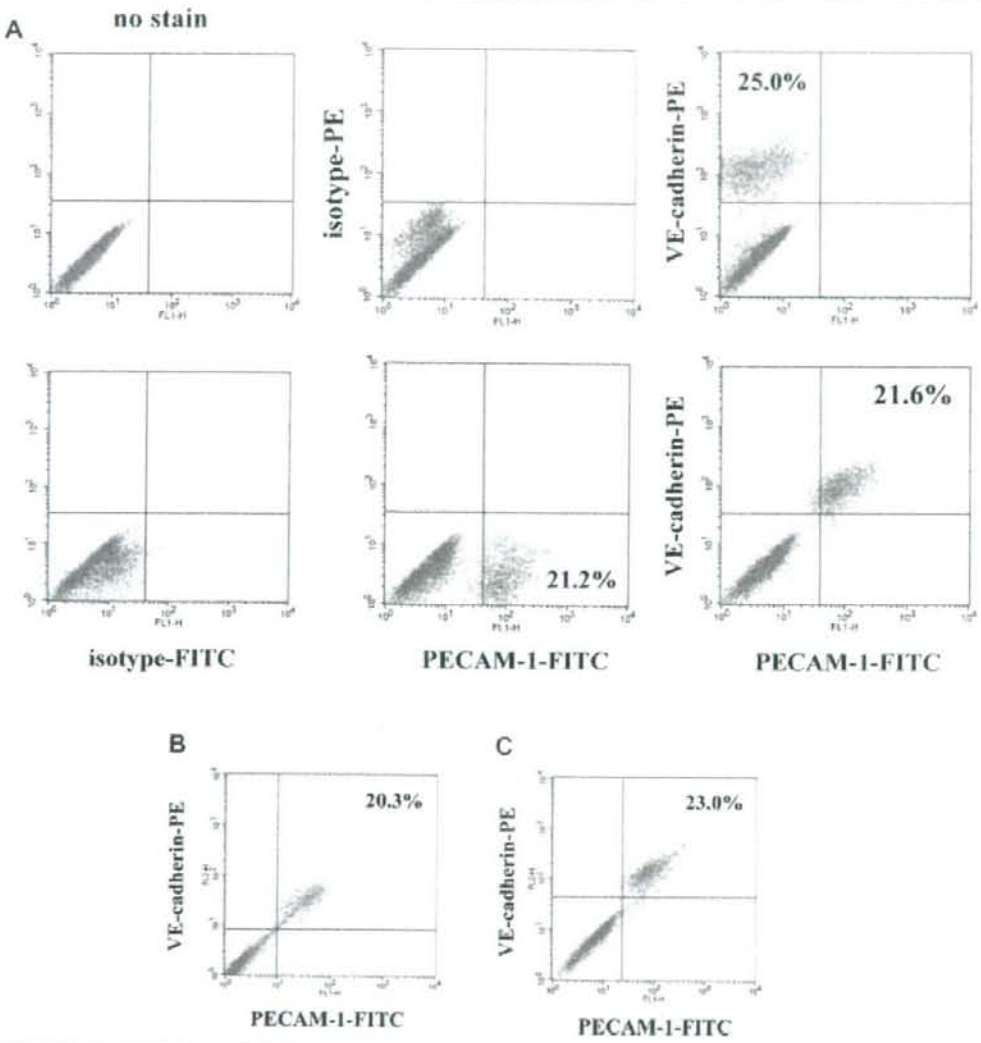

Fig. 3. Cell surface expressions of vascular endothelial markers in cmES-derived subcultured cells. A–C: Cell surface expressions of VE-cadherin and PECAM-1. The total adherent cells obtained by culture of cmES-derived spheres on gelatin-coated plates were subcultured and, after six passages (A) or eight passages (B), cells were stained by a PE-labeled anti-human VE-cadherin antibody (vertical axes), a FITC-labeled anti-human PECAM-1 antibody (horizontal axes) or each isotype control antibody as indicated. C: The total adherent cells obtained by the culture of cmES-derived spheres on gelatin-coated plates were frozen. After being thawed, cells were cultured for additional two passages and the expressions of VE-cadherin and PECAM-1 were determined by flow cytometry as in (A). D: Expressions of other endothelial markers. cmES-derived cells (ESdC), HUVEC and HAEC were subjected to flow cytometric analyses using indicated monoclonal antibodies.

(Fernandez Pujol et al., 2001; Kuwana et al., 2006), we examined the expressions of monocyte/macrophage markers of CD68, CD14 and CD11b as well as pan-leukocyte markers of CD18 and CD45. We found that the cell surface VE-cadherin-negative populations were negative for CD68 (Fig. 6K), CD14 (Fig. 6L), CD11b (Fig. 6L), CD18 (Fig. 6L), and CD45 (Fig. 6L), indicating that they are distinct from hematopoietic endothelial cell progenitors.

All those findings together suggest that our differentiation system produced almost two pure populations: cell surface VE-cadherin-positive "canonical" vascular endothelial cells and cell surface VE-cadherin-negative "atypical" vascular endothelial cells. This concept was further confirmed by the fact that neither pericytes nor undifferentiated ES cells co-existed in the differentiated samples. Pericytes are reportedly induced during vascular endothelial differentiation (Yamashita et al., 2000; Sone et al., 2003, 2007). Moreover, co-existence of pericytes, the polygonal cells, severely inhibits the expansion of vascular endothelial cells during subculture (Sone et al., 2003, 2007). In our system, however, both